DOI: 10.1002/ejic.200601091

Ten Years of a Biomimetic Approach to the Copper(II) Radical Site of Galactose Oxidase

Fabrice Thomas*[a]

Keywords: Biomimetic chemistry / Copper / Radicals / Bioinorganic chemistry / Enzyme models

An overview of recent progress in the modeling of the copper(II)-phenoxyl entity of the metalloenzyme Galactose Oxidase (GO) is presented. GO is an enzyme that is extremely engineered by nature: its active site exhibits several unusual features, such as a coordinated tyrosyl radical, post-translationally modified amino acids, and π-stacked residues. Understanding each of these particularities has posed a challenge for chemists, who have consequently developed several biomimetic complexes during the last decade. The properties of representative complexes are described herein, with special emphasis given to copper(II) complexes involving tripodal ligands. All these biomimetic compounds have been developed with the aim of better understanding biologically relevant problems. I show here that the structural attributes, reactivity, electronic properties, self-processing, and many other properties of GO can be addressed successfully using model complexes.

Introduction

Various strategies are used by metalloproteins to store and transfer electrons in biochemical processes.[1] In the simplest case, the number of metal ions required for the reaction matches the number of electrons to be transferred. This is illustrated by tyrosinases that catalyze the hydroxylation of phenols, which have an active site that contains two copper ions. An organic cofactor could also complete the metal-driven electron transfer, as in copper amine oxidases that catalyze the oxidative deamination of amines using topaquinone. It has been shown recently that some metalloenzymes are able to generate an organic radical cofactor directly on their own peptidic chain to complete metal-driven electron transfers.[2,3] Galactose oxidase (GO), whose active site includes a tyrosyl radical coordinated to a copper(II) ion, is a prototypical enzyme of this class and is a fascinating example of synergy between a metal and a radical to perform oxidation reactions. The metal-radical array in these systems is much more than an association, and the advantage of maintaining a tyrosyl radical close to the metal ion is that hydrogen abstraction from a C–H bond by radicals is energetically favored over a hydrogen atom transfer to an inorganic metal-based oxidant (the thermodynamic affinity of a tyrosyl radical for a hydrogen atom is high).[4] The tyrosyl radical in GO thus performs the hydrogen atom abstraction while the metal ion is involved in a classical single electron transfer. GO is an enzyme that is extremely engineered by nature: its active site exhibits several unusual features such as post-translationally modified amino acids and π-stacked residues, and understanding each of these particularities poses a challenge for biologists and chemists alike. In studies aimed at understanding this enzyme, biochemists commonly use directed mutagenesis while chemists use a biomimetic approach. The latter consists of synthesizing and characterizing abiotic compounds that exhibit some or all of the enzyme's features. The devel-

[a] Département de Chimie Moléculaire – Chimie Inorganique Redox Biomimétique (CIRE) UMR CNRS 5250, Université Joseph Fourier,
B. P. 53, 38041 Grenoble cedex 9, France
Fax: +33-4-76514836
E-mail: Fabrice.Thomas@ujf-grenoble.fr

Fabrice Thomas was born in 1973. He did his undergraduate studies in Biochemistry at the University of Grenoble, where he received his Ph.D. degree in Molecular Chemistry in 1999. He then spent one year at the Institute of Physics at the University of Lübeck (Germany) as a postdoctoral fellow supervised by Prof. Trautwein. He worked on the characterization of iron centers in metalloproteins and models by Mössbauer spectroscopy. He is currently assistant professor in the Department of Molecular Chemistry, in the Inorganic Redox Biomimetic Chemistry team (CIRE) at the University of Grenoble. His main research interests are in the areas of inorganic and biomimetic chemistry. More specifically, he works on the metal-radical association in complexes that are bio-inspired by galactose oxidase.

opment of mimics of GO began in 1996, and has contributed significantly to an enhanced understanding of the spectral properties, structural attributes, and even reactivity of its active site. Two reviews concerning the first-generation models of both the active Cu^{II}-phenoxyl and inactive Cu^{II}-phenolate forms of the GO active site[5,6] appeared in the literature in 2000.

Several complexes involving phenoxyl moieties coordinated to other divalent metal ions, or even trivalent metal ions, have also been synthesized. Many of these have been described by Wieghardt et al., and were reviewed in 2001.[7] These studies gave a lot of insights into the properties of coordinated phenoxyl radicals. More recently, a review focused on the aerobic oxidation of various substrates catalyzed by copper and manganese radical complexes has been published by the same group.[8] In this review I will briefly present the literature prior to 2000 and then focus my attention on more recent Cu^{II}-phenoxyl complexes. As a preamble, an overview of the biochemical properties of the GO active site is given. I then describe the properties of representative complexes that have been used as models of GO, with special emphasis on copper(II) complexes involving tripodal ligands, as their rich chemistry has been extensively studied by several groups. Next, I present the biologically relevant problems that have been addressed and solved by biomimetic studies, and finally I describe GO-inspired systems dedicated to the storage of three oxidizing equivalents (i.e. complexes containing either two phenoxyl radicals coordinated to a single copper ion, or a single phenoxyl radical coordinated to two copper ions).

Galactose Oxidase

The most important aspects of GO chemistry have been recently reviewed, so only a brief presentation of the essential facts will be given here.[9–11] Galactose oxidase is an extracellular type II mononuclear copper protein (68 kDa) of fungal origin. GO catalyses the two-electron oxidation of a wide range of primary alcohols to their corresponding aldehydes with the concomitant reduction of molecular oxygen to hydrogen peroxide. The apparent paradox − a two-electron oxidation performed by a single copper ion − is explained by the involvement of another redox center, namely a tyrosyl radical from the protein, during the catalytic cycle. The physiological role of GO is not clear, although it could be involved in the production of H_2O_2 for further use as an co-oxidant for lignin- and cellulose-degrading peroxidases and could also provide an antibiotic defense within the rhizosphere.[10]

Structure of the Active Site

GO has been crystallized and its X-ray crystal structure was reported about ten years ago (Figure 1).[12,13] Its active site comprises a copper atom in a distorted square-based pyramidal geometry with Tyr495 occupying the axial position. His581, His496, Tyr272, and an exogenous ligand (H_2O or acetate, replacing the substrate) coordinate the copper in equatorial positions. The most striking feature of this complex is the cross-linking of Tyr272 to Cys228 through a thioether bond at the *ortho* position of the OH group, which presumably lowers the tyrosyl/tyrosine redox potential. The indole ring of Trp290 is π-stacked with Tyr272 and is believed to control the access to the active site and shield the Cys-Tyr cofactor from exposure to solvent. The enzyme can exist in three well-defined oxidation levels: the Cu^{II}-tyrosyl radical oxidized form, an intermediate Cu^{II}-tyrosinate form, and the reduced Cu^{I}-tyrosine form. Only the former and latter forms are catalytically active. The Cu^{II}/Cu^{I} redox couple has been estimated to be –0.24 V vs. Fc^+/Fc at pH 7,[14,15] while the tyrosyl/tyrosinate one has been estimated to be 0.01 V vs. Fc^+/Fc. The Cu^{II}-tyrosyl radical and the fully reduced copper(I) form undergo a rapid bimolecular comproportionation that affords the catalytically inactive Cu^{II}-tyrosinate form.[15]

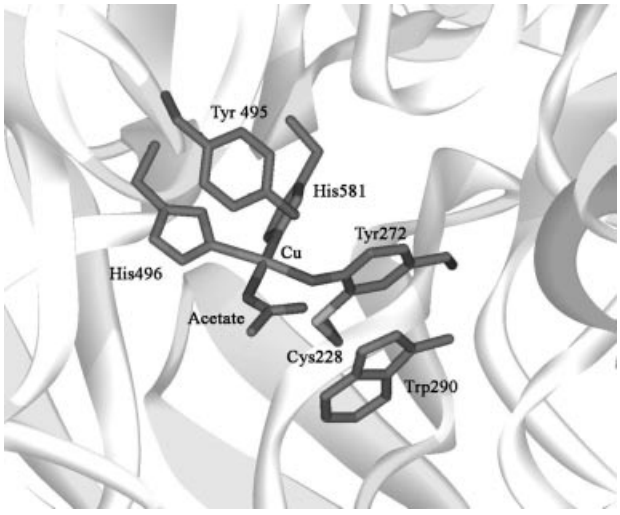

Figure 1. X-ray crystal structure of the active site of GO (adapted from ref.[12]).

The Cu^{II}-tyrosinate form possesses spectroscopic signatures that are typical of mononuclear copper(II) complexes, while the reduced form is EPR-silent and colorless. Extensive spectroscopic studies on the active oxidized form have shown that the radical is mainly harbored by the equatorially bound Tyr272 residue. Strong antiferromagnetic exchange coupling between the tyrosyl radical and the paramagnetic copper(II) ion results in a diamagnetic ground state, with a singlet–triplet splitting greater than 200 cm^{-1}.[16] A value of 752 cm^{-1} has recently been reported from TD DFT calculations.[17] GO exhibits an unusually intense optical spectrum with absorption bands at around 445 and 800 nm[18] that are assigned to π–π* transitions of the tyrosyl radical.[9–11,17] The enzyme is relatively stable in this form, with a half life ($t_{1/2}$) of 7.2 days for its self-decomposition.[19]

Free Radical Catalysis

Catalysis by GO proceeds according to a ping-pong turnover reaction.[18,19] In the first half-reaction the alcohol substrate binds to the oxidized Cu^{II}-radical active site and reduces both redox centers [tyrosyl radical and copper(II) ion], and the aldehyde product is released. This aldehyde product, which has a low affinity for the complex, is then released into the medium. In the second half-reaction, the Cu^{I}-tyrosine site binds O_2 and reduces it to H_2O_2, thus regenerating the initial Cu^{II}-tyrosyl radical state. A proposed catalytic mechanism is shown in path A of Figure 2.[9–11,18–21]

The catalysis is initiated by a weak (almost collisional) association with the substrate. The structure of GO reveals a shallow channel through which substrates bound by Phe194, Phe464, Arg330, and Trp290 reach the catalytic site. Reaction over a wide range of concentrations shows that the enzyme is saturable with a dissociation constant of 71 mM for the formation of the initial complex with D-galactose.[10] This low affinity, which is a consequence of a quite open active site, is consistent with a lack of substrate selectivity. In contrast, the enzyme strictly constrains the orientation of the substrate in its active site, thereby allowing a stereospecific abstraction of the pro-*S* hydrogen by the nearby tyrosyl radical. Modeling galactose coordinated to the copper(II) ion of the native enzyme shows that the pro-α-*S*-hydrogen is located at a hydrogen-bonding distance from Tyr272 (ca. 2.5 Å), while the pro-*R* hydrogen is away from the pro-radical cofactor.[11] The steric constraints that lead to this stereoselectivity are not limited to galactose, as similar selectivity as been demonstrated for any substrate bearing a branched β-C. After binding of the substrate to the copper equatorial position, the first step involves a proton transfer (step 1, Figure 2).[22] Deprotonation of the alcohol is facilitated by copper coordination and a short H-OTyr495 bond (estimated to be around 2.8 Å).[23] This process occurs with a low barrier (nearly isothermic), on a nanosecond timescale, due to the optimized hydrogen-bonding geometry and the close matching of tyrosine pK_a and coordinated alcohol pK_a. Two crucial facts result from this first step: the Cu^{II}–substrate interaction is strengthened and the C–H bond energy of the deprotonated substrate is lowered by 10 kcal mol^{-1}. The second step involves a hydrogen-atom transfer from the alkoxide substrate to the equatorial Tyr272 radical (step 2, Figure 2). This is the major rate-limiting step (at high O_2 concentrations) in the whole catalytic pathway, as reflected by the

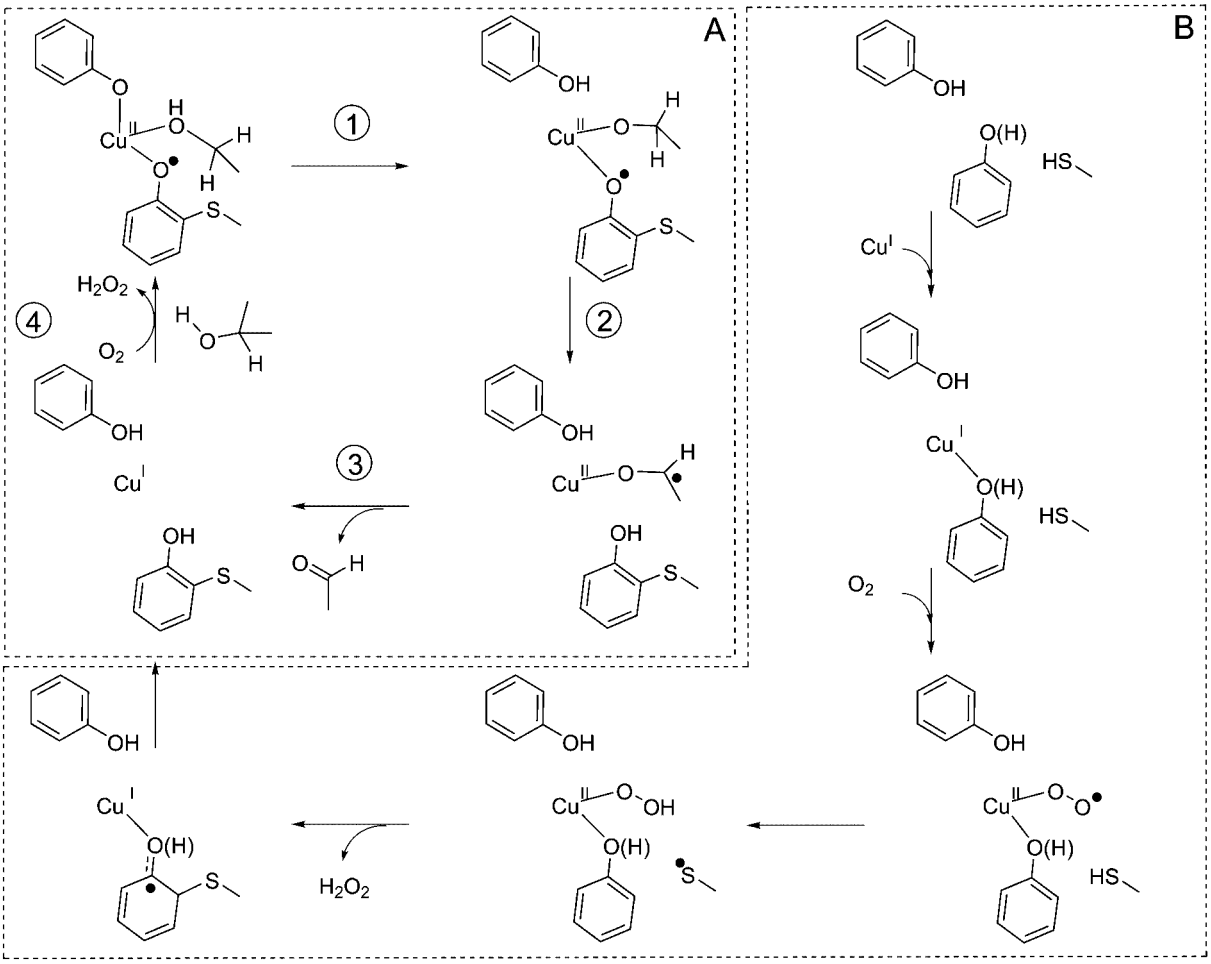

Figure 2. Free radical catalysis by mature GO (A) and self-processing of the pre-form of GO (B) (adapted from ref.[19,30] respectively).

large kinetic isotope effect (KIE) of 7.7 for D-galactose (an even larger KIE of 22 has been reported for 1-*O*-methyl-α-D-galactopyranoside)[18] and the fact that GO remains essentially fully oxidized during turnover. The large non classical KIE of 22 as well as a strong temperature dependence of the KIE are clear evidence of the tunneling of a hydrogen atom in the rate-limiting step.

The free activation energy for hydrogen abstraction has been estimated to be 13.6 kcal mol^{-1}. An optimized structure for the transition state can be obtained from B3LYP calculations:[23] it has a five-atom cyclic structure in which the O–H bond length is 1.24 Å while the C–H bond length is stretched to 1.36 Å. The hydrogen atom is then transferred perpendicularly to the phenol ring plane, in agreement with a π character of the radical. Mechanism-based inactivation of GO by ultrafast radical probes confirms that a short-lived substrate ketyl radical anion results from the H-abstraction (hydrogen abstraction is rate limiting).[24] The ketyl radical then reduces the metal center (single-electron transfer; step 3, Figure 2) and is released to allow O_2 binding (step 4, Figure 2).[9–11,18–21,25]

Quantitative structure–activity relationship correlations using the steady-state rate data for the oxidation of benzyl alcohol derivatives have revealed that the three elementary events, namely proton transfer, single electron transfer, and hydrogen-atom abstraction, are asynchronous components of the whole catalytic process rather than distinct kinetic intermediates.[26,27] The difficult-to-oxidize nitro derivatives as well as pyranosides and physiological substrates exhibit a large substrate KIE associated with a negligible solvent KIE: C–H bond cleavage (hydrogen-atom abstraction) is here fully rate limiting. In contrast, the easier-to-oxidize methoxybenzyl alcohols exhibit a smaller substrate KIE and a non-negligible solvent KIE, thus reflecting a small proton transfer contribution in the transition state and a pronounced single electron transfer character for substrate oxidation.

The re-oxidation step of GO (step 4, Figure 2) is a remarkable example of two-electron chemistry catalyzed by dioxygen, as the ratio of superoxide released does not exceed one for 2000 turnovers. Kinetic data have shown that re-oxygenation of the GO active site occurs with a rate constant of around 8×10^6 M^{-1} s^{-1} at 277 K.[18] However, the high instability of the oxygenated complex makes this step much less certain than the former, in spite of a main role for the enzyme being formation of hydrogen peroxide.

Radical Cofactor Formation

GO is a secretory protein, which means that its maturation requires several successive steps: cleavage of a signal sequence that directs translocation, metal binding, and cofactor processing. The structure of a metal-free unprocessed pre-form of the protein has been described recently.[28] Its active site does not contain the Cys-Tyr cross-link, and Cys228 has been found oxidized into a sulfenic acid. This latter modification likely arises from oxidative damage to the protein. Conversion of this pre-form into the catalytically active form appears to be a self-processing event that requires only copper and O_2.[29] Copper in both oxidation states induces cross-linking and radical cofactor formation, but with very different time scales [$t_{1/2}$ = 3.9 s at pH 7 with copper(I) and 5.1 h with copper(II)]. The Cu^I-dependent biogenesis reaction may thus more closely resemble the physiological process.[30] A mechanism for this reaction, which involves initial copper(I) binding to the pre-form to afford a trigonal copper(I) complex that reacts with O_2, has been proposed recently (Figure 2, B). The resulting species is a reactive Cu^{II}-$O_2^{\cdot-}$ compound that abstracts a hydrogen atom from Cys228 and releases H_2O_2. The thiyl radical then attacks the ε-C ring carbon of Tyr272, and rearomatization occurs by proton and electron transfer to the metal. At this stage, the fully reduced form of the mature GO is obtained. This then readily undergoes two-electron oxidation by O_2 to give the catalytically active Cu^{II}-tyrosyl radical form of the enzyme and H_2O_2.

Main Classes of Model Compounds for the GO Active Site

The discovery of a Cu^{II}-phenoxyl radical entity in the GO active site has stimulated a number of chemists to incorporate this unknown unit in coordination complexes. For phenoxyl radicals to exist as more than a transient intermediate in solution, the *ortho* and *para* positions of the phenol must be blocked by groups that give increased steric protection or resonance stabilization.[31] The phenoxyl radicals are strongly colored − they exhibit characteristic absorption bands in the regions between 400 and 450 nm and above 600 nm that are attributed to π–π* transitions − which makes them easy to detect.[32] During the last decade many efforts have thus been made to incorporate such modified phenols in ligands, leading to the isolation of complexes able to model (functionally or structurally) the GO active site. The main ligand scaffolds developed will be listed below, together with the general properties of the corresponding copper(II) complexes. The following nomenclature will be used: H_xL^y for a ligand y possessing x acido-basic sites and $[Cu(H_xL^y)(X)_z]$ for the copper(II) complex of H_xL^y bearing z coordinated exogenous ligands (X being an anion or solvent molecule). For clarity, the overall charge of the ligands and complexes is omitted. When the oxidation number of the copper ion is not indicated it is +2.

Salen Ligands

A wide number of copper(II) complexes of salen-type ligands have been described so far, therefore the discussion here will be limited to general considerations and complexes specifically designed to model the GO active site,[33–43] in other words those bearing a sterically bulky substituent at the *ortho* and *para* positions of each phenol to prevent bis(μ-phenolate) dimer formation and to stabilize a phenoxyl radical (Figure 3). The copper(II) ion in these com-

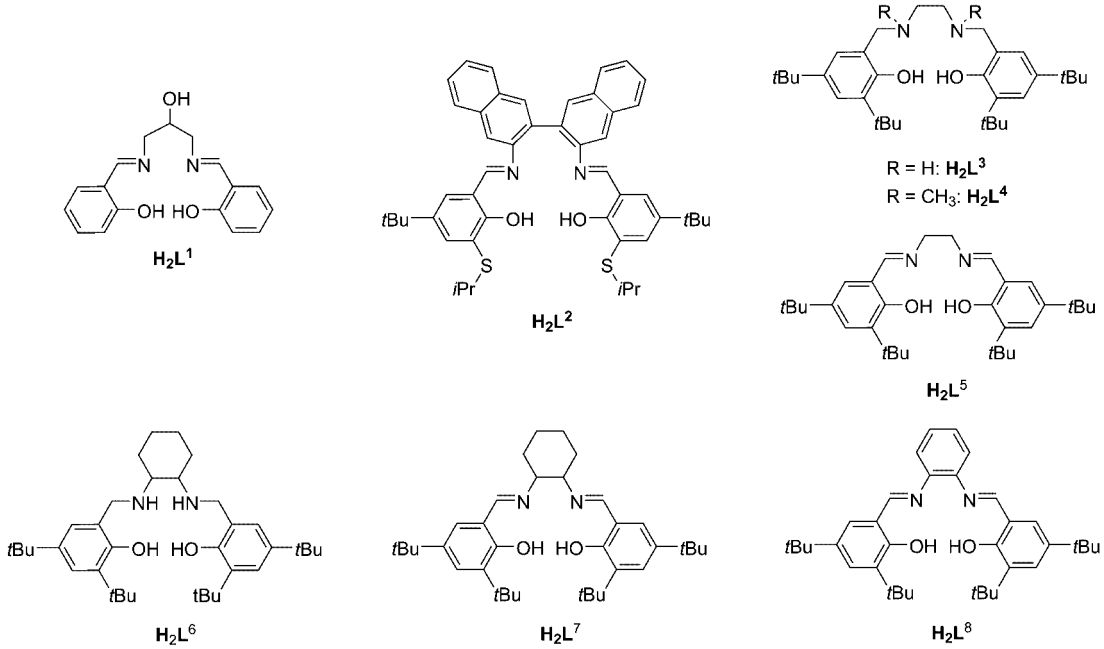

Figure 3. Salen-based ligands: H_2L^1 (ref.[33]), H_2L^2 (ref.[34,35]), H_2L^3 (ref.[36,37]), H_2L^4 (ref.[38]), H_2L^5 (ref.[37]), H_2L^6 (ref.[39,40]), H_2L^7 (ref.[37,39,40]), H_2L^8 (ref.[37]).

plexes is tetracoordinate in a square planar or tetrahedral geometry, as shown by their X-ray crystal structures and EPR spectroscopy. The flexibility and degree of distortion from square planar towards a tetrahedral geometry can be modulated by the nature of the linker between each salicylidene moiety. The electrochemical behavior of salen complexes is characterized by two oxidation waves at potentials higher than 0.3 V vs. Fc^+/Fc {$[Cu(L^2)]$,[34,35] $[Cu(L^5)]$,[37] $[Cu(L^7)]$,[37,39,40] and $[Cu(L^8)]$[37]}, corresponding to the successive formation of mono- and bis(phenoxyl) radical species (Table 1). The reduced salen complexes {$[Cu(L^{3,4})]$[36–38] and $[Cu(L^6)]$[39,40]} exhibit a similar oxidative behavior, although they are much more easily oxidized. On a spectroscopic point of view, the UV/Vis spectra of the salen complexes is dominated by intense charge-transfer (CT) transitions at around 400 nm ($\varepsilon > 8000\ M^{-1}cm^{-1}$), while the reduced salens exhibit a much less intense phenolate-to-copper CT ($\varepsilon < 2000\ M^{-1}cm^{-1}$). Both exhibit low intensity copper(II) d–d transitions at wavelengths higher than 500 nm. Upon one-electron oxidation, the highest intensity bands of the salen complexes are shifted towards higher wavelengths (Table 1). The UV/Vis spectra of the Cu^{II}-phenoxyl complexes of reduced salen complexes are more similar to those of uncoordinated phenoxyl radicals, with classical π–π* transitions at around 400–450 and 600–700 nm (Table 1). Stack et al. have also measured the NIR

ATable 1. Properties of some Cu^{II}-phenoxyl radical complexes of salen ligands.

Complex	$E_{1/2}$[a]	UV/Vis[b]	Solvent	Ref.
$[Cu(L^1)]$	n.d.	370 (11300), 611 (263)	DMF	[33]
$[Cu(L^2)]$	0.62	n.d.	CH_3CN	[34,35]
$[Cu(L^3)]$	0.11, 0.45	410 (1880), 594 (900)	CH_2Cl_2/DMSO	[36,37]
$[Cu(L^4)]$	0.16, 0.32	450 (1960), 650 (1370)	CH_2Cl_2	[38]
$[Cu(L^5)]$	0.31, 0.79	306 (4160), 405 (11440), 500 sh (820)	CH_2Cl_2	[37]
$[Cu(L^6)]$	0.08, 0.21	n.d.	CH_2Cl_2	[39,40]
$[Cu(L^7)]$	0.45, 0.65	376 (12400), 565 (600)	CH_2Cl_2	[37,39,40]
$[Cu(L^8)]$	0.65, 0.83	402 (17750), 445 (24600)	CH_2Cl_2	[37]
Complex[c]	EPR signal[d]	UV/Vis[b]	Solvent	Ref.
$[Cu(L^{2\cdot})]$	silent (77 K)	featureless	CH_3CN	[34,35]
$[Cu(L^{3\cdot})]$	silent (4 K)	384 (4050), 626 (3310)	CH_2Cl_2/DMSO	[36,37]
$[Cu(L^{5\cdot})]$	silent (4 K)	370 (11760), 552 (7250)	CH_2Cl_2	[37]
$[Cu(L^{6\cdot})]$	silent (77 K)	413 (3000), 527 (3100), 607 (3400)	CH_2Cl_2	[39,40]
$[Cu(L^{6\cdot\cdot})]$	signal at $g = 2$	405 (5800), 418 (5800), 476 sh, 592 (1300)	CH_2Cl_2	[39,40]
$[Cu(L^{7\cdot})]$	silent (4 K)	345 (11400), 558 (5500), 1750 (2400)	CH_2Cl_2	[37,39,,40]
$[Cu(L^{7\cdot\cdot})]$	$S = 3/2$	354 (8170), 380 sh (7510), 443 (10700), 562 br. (2030), 800 br. (2010)	CH_2Cl_2	[37,39,40]
$[Cu(L^{8\cdot})]$	silent (4 K)	444 (21800), 577 (3530)	CH_2Cl_2	[37]
$[Cu(L^{8\cdot\cdot})]$	$S = 3/2$	420 (16600), 446 (18900), 550 sh (4500), 900 br. (4300)	CH_2Cl_2	[37]

[a] V vs. Fc^+/Fc. [b] λ [nm] (ε [$M^{-1}cm^{-1}$]). [c] The properties of the one-electron-oxidized forms of $[Cu(L^1)]$ and $[Cu(L^4)]$ are not reported. [d] X-band. The Cu^{II}-phenolate complexes exhibit an $S_{Cu} = ½$ signal.

spectra of [Cu($L^{6\cdot}$)] and [Cu($L^{7\cdot}$)] and found intense transitions at 1600 and 1750 nm, respectively, attributed to phenolate-phenoxyl charge transfers.[39,40] All the Cu^{II}-monophenoxyl radical complexes were found to be EPR-silent as the result of a magnetic coupling between the coordinated radical and the metal spins.

The first use of salen copper(II) complexes to mimic the reactivity of GO towards alcohol oxidation was reported in 1986 by Katajima et al.[33] Unfortunately, no evidence for a "true" GO-like reactivity, such as phenoxyl radical formation, was shown in the reaction of the copper(II) complex of H_2L^1 with alcohols.[33] Stack et al. revisited these kinds of complexes 10 years later. He reported that the copper(II) complex of H_2L^1 is able to catalyze the aerobic oxidation of benzyl alcohol into benzaldehyde with high turnovers (1300 at 295 K in 20 h).[34,35] The ligand structure was improved to achieve such reactivity: the phenolate moieties were *ortho*- and *para*-substituted by electron-donating groups to stabilize the phenoxyl radical, and a significant tetrahedral distortion was induced around the copper atom [thus stabilizing the copper(I) ion] by using a binaphthyl linker. They showed experimentally that the active species is the Cu^{II}-phenoxyl form of the complex. The substrate adduct was a five-coordinate square-pyramidal Cu^{II}-phenoxyl complex (further theoretical studies on its reactivity are presented below). Oxidation of the initial Cu^{II}-phenolate complex into the catalytically active Cu^{II}-phenoxyl radical species, however, requires addition of a strong oxidant. For this reason we have synthesized the copper(II) complex of the reduced salen ligand H_2L^3.[36,37] This complex is much more readily oxidizable, as judged by its redox potential, which is around 0.5 V lower than for Stack's model complex (Table 1). The Cu^{II}-phenoxyl complex leads to the oxidation of several unactivated primary alcohols (such as methanol) into aldehydes in the presence of catalytic amounts of base; secondary alcohols are not affected.[36] More recently, copper(II) complexes of reduced salen ligands have also been described by Palaniandavar et al. (H_2L^4)[38] as well as Stack et al.[39,40] [Cu(L^6)], for instance, was shown to model the acceleration of the reaction rate by substrate binding as does GO. Its "true" salen complex derivative [Cu(L^7)], however, does not exhibit such reactivity. In another approach, we focused our interest on developing planar scaffolds such as H_2L^5 and H_2L^8 to stabilize copper(II) coordinated bis(phenoxyl) radicals.[37] The Cu^{II}-phenoxyl radical complex of [Cu($L^{8\cdot}$)] has been further utilized by other groups[41] for different purposes.[42] A pentadentate reduced salen ligand, which could be oxidized into a Cu^{II}-phenoxyl radical species, as shown by its EPR-silence and π–π* transitions at 390 and 408 ($\varepsilon > 1000\ M^{-1}cm^{-1}$) and 600–900 nm ($\varepsilon < 1000\ M^{-1}cm^{-1}$), has also been described by Neves et al.[43]

Imino-, Thio-, and Semiquinonate Ligands

Wieghardt et al.[44–51] have contributed widely to the development of an extraordinary class of model compounds for GO that involves imino-, thio-, and semiquinonate ligands (Figure 4). These are much more easily oxidizable (the phenolate oxidation potentials are negative vs. Fc^+/Fc, which makes them oxidizable by air; Table 2) than other classes of ligands, and are so stable in their radical form that structural characterization could be envisaged. Some of these complexes were also found to be efficient catalysts for the aerobic oxidation of alcohols. Mixing the tridentate ligand H_2L^9 with copper(II) in the presence of triethylamine and air affords the EPR-silent dinuclear Cu^{II}-phenoxyl complex [Cu($L^{9\cdot}$)]$_2$, which exhibits absorption bands at 408 and 650 nm (Table 2).[44] The mononuclear Cu^{II}-phenoxyl complex [Cu($L^{10\cdot}$)(NEt_3)] was obtained under similar conditions by replacing H_2L^9 with H_3L^{10} and structurally characterized.[45] The tridentate ligand is coordinated to a single copper(II) ion and the fourth coordination site is occupied by an NEt_3 molecule. This complex is also EPR-silent as a result of an antiferromagnetic coupling between the radical and the metal spin (J estimated at $-137\ cm^{-1}$). Both [Cu($L^{9\cdot}$)]$_2$ and [Cu($L^{10\cdot}$)(NEt_3)] were found to be very efficient catalysts for the aerobic oxidation of alcohols. Interestingly, treatment of a solution of copper(I) and H_3L^{10} neutralized by NEt_3 with pure dry O_2 yielded crystals of a copper(II) complex containing a bound superoxide ion, an intermediate suggested in the catalytic pathway of GO. Recently, H_2L^{11}, the selenium analogue of H_2L^9, has been described.[51] This ligand reacts with copper ions in the pres-

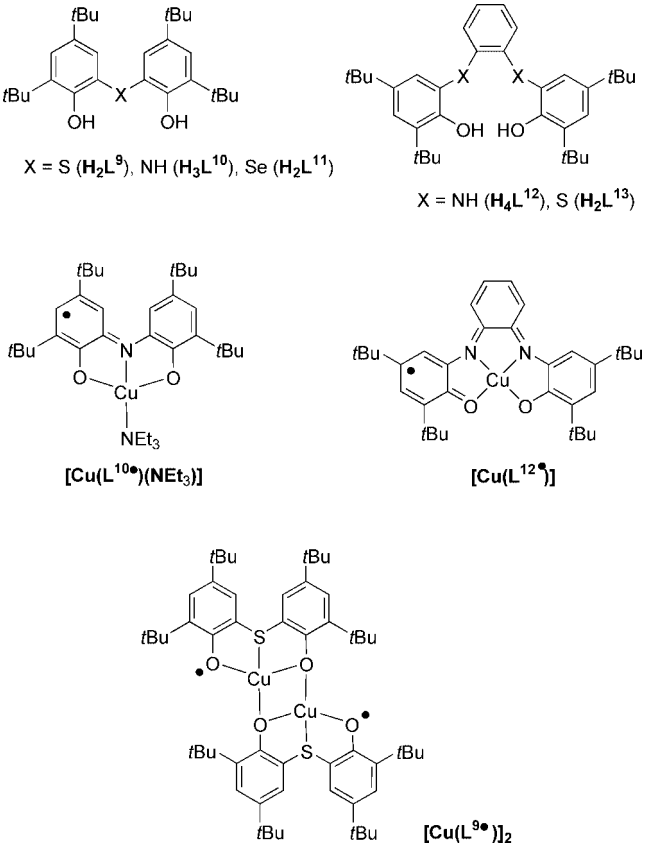

Figure 4. Thioiminosemiquinone ligands and their copper(II) complexes: H_2L^9 and [Cu($L^{9\cdot}$)]$_2$ (ref.[44]), H_3L^{10} and [Cu($L^{10\cdot}$)(NEt_3)] (ref.[45]), H_2L^{11} (ref.[51]), H_4L^{12} and [Cu($L^{12\cdot}$)] (ref.[46]), H_2L^{13} (ref.[48]).

Table 2. Properties of some copper(II) complexes of imino- and thiosemiquinone ligands.

Complex	$E_{1/2}$[a]	EPR signal[b]	UV/Vis[c]	Solvent	Ref.
$[Cu(L^{9\cdot})]_2$	–1.26,[d] –0.29[d]	$S = 0$	400 sh, 408 (8000), 424 sh, 650 (660)	CH_2Cl_2	[44]
$[Cu(L^{10\cdot})(NEt_3)]$	–1.06,[d] –0.14[d]	$S = 0$	n.d.	CH_2Cl_2	[45]
$[Cu(L^{12\cdot})]$	–1.42,[d] –0.66,[d] –0.06,[d] 0.41	$S = 0$	320 (5100), 478 (6400), 981 (1200)	CH_2Cl_2	[46]
$[Cu(L^{13\cdot})]$	0.62 (irr), 0.99 (irr)[e]	unstable	unstable	CH_2Cl_2	[48]

[a] V vs. Fc^+/Fc. [b] X-band. [c] λ [nm] (ε [$M^{-1}\,cm^{-1}$]). [d] Reduction waves. [e] Irreversible processes. The potentials correspond to the E_p^a values obtained from the cyclic voltammetry curve of $[Cu(L^{13})]$.

ence of different amines to give rise to a variety of mono-, di-, and even trinuclear complexes that exhibit distinct reactivities towards alcohol oxidation.

The coordinated tetradentate ligand H_4L^{12} can exist in five oxidation levels (each of which has been fully characterized), two of which are paramagnetic monoradicals and another is a diamagnetic diradical.[46] $[Cu(L^{12\cdot})]$ (and its zinc analog) selectively oxidizes primary alcohols in a stoichiometric fashion under anaerobic conditions to yield the corresponding aldehyde and a protonated form of the two-electron-reduced catalyst. This latter complex can reduce molecular dioxygen into H_2O_2, thus regenerating $[Cu(L^{12\cdot})]$. This makes oxidation of alcohols into aldehydes catalytic under aerobic conditions. H_2L^{13}, the sulfur analogue of H_2L^{12}, has been described along with its copper(II) complexes.[48] Electrochemical experiments showed that the coordinated *o*-thioetherphenolate moieties could be oxidized into phenoxyl radicals. Unfortunately, the oxidized species are very unstable and do not allow further spectroscopic characterization.

TACN Ligands

The macrocycle 1,4,7-triazacyclononane (TACN) coordinates one metal ion through its three amine groups and can be further derivatized to incorporate one, two, or three additional coordinating groups such as phenols (Figure 5). Many mono- and bis(phenolate) copper(II) complexes have been structurally characterized that show a five-coordinate copper(II) ion in a slightly distorted square-pyramidal geometry. A coordination number of six can be achieved by addition of exogenous bidentate ligands such as Ph_2acac.[52] In all of the structures the phenolate donor(s) reside(s) in the equatorial plane (*cis* to each other if two are present), while one amine nitrogen coordinates weakly in the axial position.

Tolman et al. reported one of the first model compounds for the Cu^{II}-radical site of GO using this TACN framework, namely the copper(II) complex $[Cu(L^{15})(CH_3CN)]$, in 1996.[53,54]. Its Cu^{II}-phenoxyl radical form was found to be relatively stable in CH_2Cl_2, as judged in the cyclic voltammograms by the reversible signal at 0.31 V (vs. Fc^+/Fc) obtained for the phenoxyl/phenolate redox couple. It is EPR-silent as the result of a magnetic coupling between the radical and the metal. No more phenolate-to-copper CT transitions are observed at 538 nm in the radical complex $[Cu(L^{15\cdot})(CH_3CN)]$. Instead, absorption bands typical for

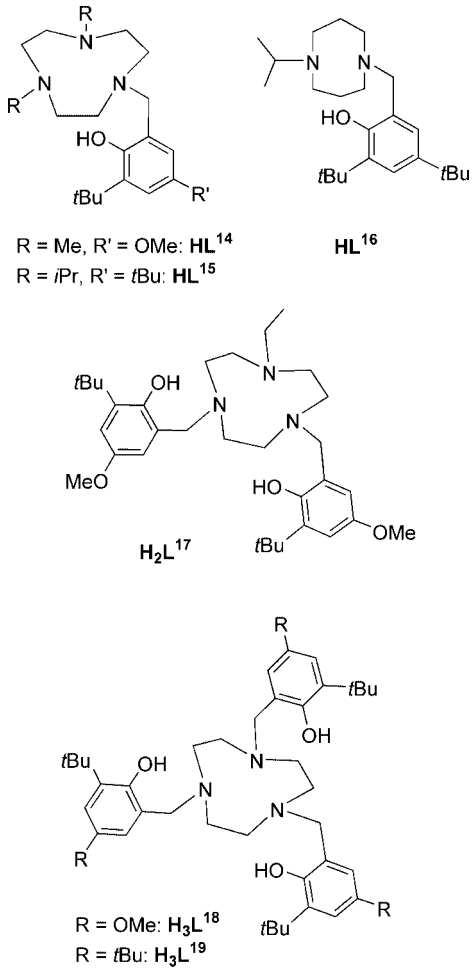

Figure 5. Ligands based on the TACN scaffold: HL^{14} (ref.[52]), HL^{15} (ref.[53,54]), HL^{16} (ref.[55]), H_2L^{17} (ref.[57]), $H_3L^{18,19}$ (ref.[56]).

phenoxyl radicals are observed at 410 and 672 nm (Table 3). The benzyl alkoxide adduct $[Cu(L^{15})(benzyl\ alkoxide)]$ has been crystallized and shows an $O_{phenolato}\cdots H–C_{substrate}$ interaction similar to that proposed for GO during enzyme turnover. More recently, the Cu^I-phenolate complexes of HL^{15} and HL^{16} have been isolated with the aim of modeling the reduced form of the GO active site.[55] Their reactivity towards molecular dioxygen will be discussed below.

This TACN scaffold has been developed concomitantly by Wieghardt et al.: the Cu^{II}-bis(phenolate) complex $[Cu(L^{17})]$ and its counterpart phenol-phenolate complex $[Cu(HL^{17})]$ could be isolated from the ligand H_2L^{17}.[57] The CV curves of $[Cu(L^{17})]$ exhibit two ligand-centered oxi-

Table 3. Properties of some Cu^{II}-phenoxyl radical complexes of TACN ligands.

Complex	$E_{1/2}$[a]	UV/Vis[b]	Solvent	Ref.
[Cu(L^{14})(Ph_2acac)]	–0.33	334 (16700), 358 (16400)	CH_2Cl_2	[52]
[Cu(L^{15})(CH_3CN)]	0.31	342 (3600), 538 (1440), 660 sh (600)	CH_2Cl_2	[53,54]
[Cu(L^{17})]	–0.10, 0.14	314 (22000), 458 (1450), 698 (210)	CH_2Cl_2	[57]
[Cu(HL^{17})]	0.14	312 (7300)	CH_2Cl_2	[57]
[Cu(HL^{18})]	–0.06, 0.12	326 sh, 445 (1500), 680 br. (300)	CH_3CN	[56]
[Cu(H_2L^{18})]	0.26	321 sh, 565 br. (1200)	CH_2Cl_2	[56]
[Cu(HL^{19})]	0.15, 0.38	305 sh (11000), 348 sh, 428 (1100), 694 br. (230)	CH_3CN	[56]
[Cu(H_2L^{19})]	0.44	321 (1700), 707 sh, 822 sh	CH_2Cl_2	[56]
Complex	EPR signal[c]	UV/Vis[b]	Solvent	Ref.
[Cu($L^{14\cdot}$)(Ph_2acac)]	$S = 1$	304 (24000), 352 (22000), 412 (6100)	CH_2Cl_2	[52]
[Cu($L^{15\cdot}$)(CH_3CN)]	silent (77 K)	410 (4000), 422 sh (3800), 672 (1000)	CH_2Cl_2	[53,54]
[Cu($L^{17\cdot}$)]	silent (77 K)	309 (18000), 418 (5400), 530 (2300)	CH_2Cl_2	[57]
[Cu($HL^{17\cdot}$)]	silent (77 K)	312 (15000), 413 sh (6800), 431 (8500), 535 (1200)	CH_2Cl_2	[57]
[Cu($L^{17\cdot\cdot}$)]	$S = 3/2$	319 (24000), 431 (15000), 485 (3500)	CH_2Cl_2	[57]
[Cu($HL^{18\cdot}$)]	silent	300 (14000), 326 sh, 414 (4300), 600 sh	CH_3CN	[56]
[Cu($H_2L^{18\cdot}$)]	silent	300 (21000), 328 sh, 411 (6100), 432 (7600)	CH_2Cl_2	[56]
[Cu($HL^{19\cdot}$)]	silent	387 sh, 402 (2800), 420 sh, 548 br. (1400),	CH_3CN	[56]
[Cu($H_2L^{19\cdot}$)]	silent	309 (10000), 407 (3600), 424 (3500), 645 br. (850)	CH_2Cl_2	[56]

[a] V vs. Fc^+/Fc. [b] λ [nm] (ε [$M^{-1}cm^{-1}$]). [c] X-band. The Cu^{II}-phenolate complexes exhibit an $S_{Cu} = ½$ signal.

dation waves, while a single wave is observed for [Cu(HL^{17})] (Table 3). The electrochemically generated Cu^{II}-phenoxyl complexes [Cu($L^{17\cdot}$)] and [Cu($HL^{17\cdot}$)] are X-band EPR-silent (Table 3), which may be interpreted either by an antiferromagnetic exchange, which yields an $S_t = 0$ ground state, or large ZFS parameters of an $S_t = 1$ ground state.

The phenol-bis(phenolate) copper(II) complexes [Cu($HL^{18,19}$)] and phenolate-bis(phenol) copper(II) complexes [Cu($H_2L^{18,19}$)] have also been isolated from the ligands $H_3L^{18,19}$ (Figure 5).[56] The tris(phenol) form was found not to be stable in solution for prolonged periods. The phenol-bis(phenolate) and phenolate-bis(phenol) forms can interconvert easily by adding one equivalent of base or acid. The X-ray crystal structure of [Cu(HL^{19})] shows that one phenol unit is not coordinated to the metal ion. The CV curves of [Cu($HL^{18,19}$)] exhibit two one-electron transfer waves in the –0.06 to 0.38 V range assigned to the successive oxidation of each phenolate moiety. [Cu($H_2L^{18,19}$)], which possess a single phenolate moiety, exhibit a single wave in the 0.26–0.44 V potential range (Table 3). EPR spectroscopy reveals that [Cu($HL^{18,19\cdot}$)] and [Cu($HL^{18,19\cdot}$)], similar to [Cu($L^{17\cdot}$)] and [Cu($HL^{17\cdot}$)], are difficult to detect as they are EPR-silent (Table 3). They exhibit features in their UV/Vis spectra (Table 3) at around 400 nm (ε values ranging between 2000 and 6000 $M^{-1}cm^{-1}$) and in the 500–800 nm region (ε values lower than 1300 $M^{-1}cm^{-1}$). The intensity of the 400-nm absorption increases significantly upon protonation and its position is shifted bathochromically. This shows that protonation affects the electronic structure of the Cu^{II}-phenoxyl chromophore. The electronic hole of the phenoxyl radical in the [Cu($HL^{18,19\cdot}$)] complexes is thus proposed to be delocalized over both the phenoxyl and the phenolate moieties, whereas the spin of the unpaired electron of the phenoxyl radical is more localized on one aromatic ring in [Cu($H_2L^{18,19\cdot}$)].

Tripodal Ligands

Several research groups have adapted the well-known tripodal aromatic framework bis(pyridyl)alkylamine connected to a single phenol (N_3O donor set), or mono(pyridyl)alkylamine attached to two phenols (N_2O_2 donor set), for GO chemistry (Figure 6).[58–75] The ligand framework has been extensively studied and modulated by modifing (i) the length of the alkyl chain linking the pyridine and the pivotal nitrogen, (ii) the steric bulk provided by the *ortho* substituent of the phenol, (iii) the electronic properties of the *para* substituent of the phenol, and (iv) the basicity of the pyridine donors. A number of monomeric or dimeric complexes have been prepared from different copper(II) salts. The potential of an N_2O_2 aliphatic tripodal ligand, where the pyridine has been replaced by a primary amine and one phenol by a hydroxyl, to mimic the GO active site was explored by Hahn et al. in 2001.[76] The copper(II) complex of this ligand was isolated as a dimer that exhibits a phenolate-centered electrochemical activity. Since the coordination chemistry of tripodal aromatic ligands has been widely described during the last decade and now allows the rational design of new complexes, it will be presented in more detail than that of other ligands.

Mononuclear Cu^{II}-phenolate complexes of general formula [Cu(L^{N_3O})(X)] can be obtained from N_3O ligands in the presence of NEt_3 if the following conditions are fulfilled: large steric bulk (*tert*-butyl group) provided by the *ortho* substituent of the phenol[58,59,61] and/or use of a copper(II) salt containing a strong monoanionic donor X^-.[71,72] Many of these complexes have been structurally characterized by X-ray crystallography[58–61,64,69,71,72] and show that the copper(II) ion is pentacoordinate, with a solvent or exogenous anion that completes the N_3O donor set of the ligand (Figure 7). The phenolate donor can bind

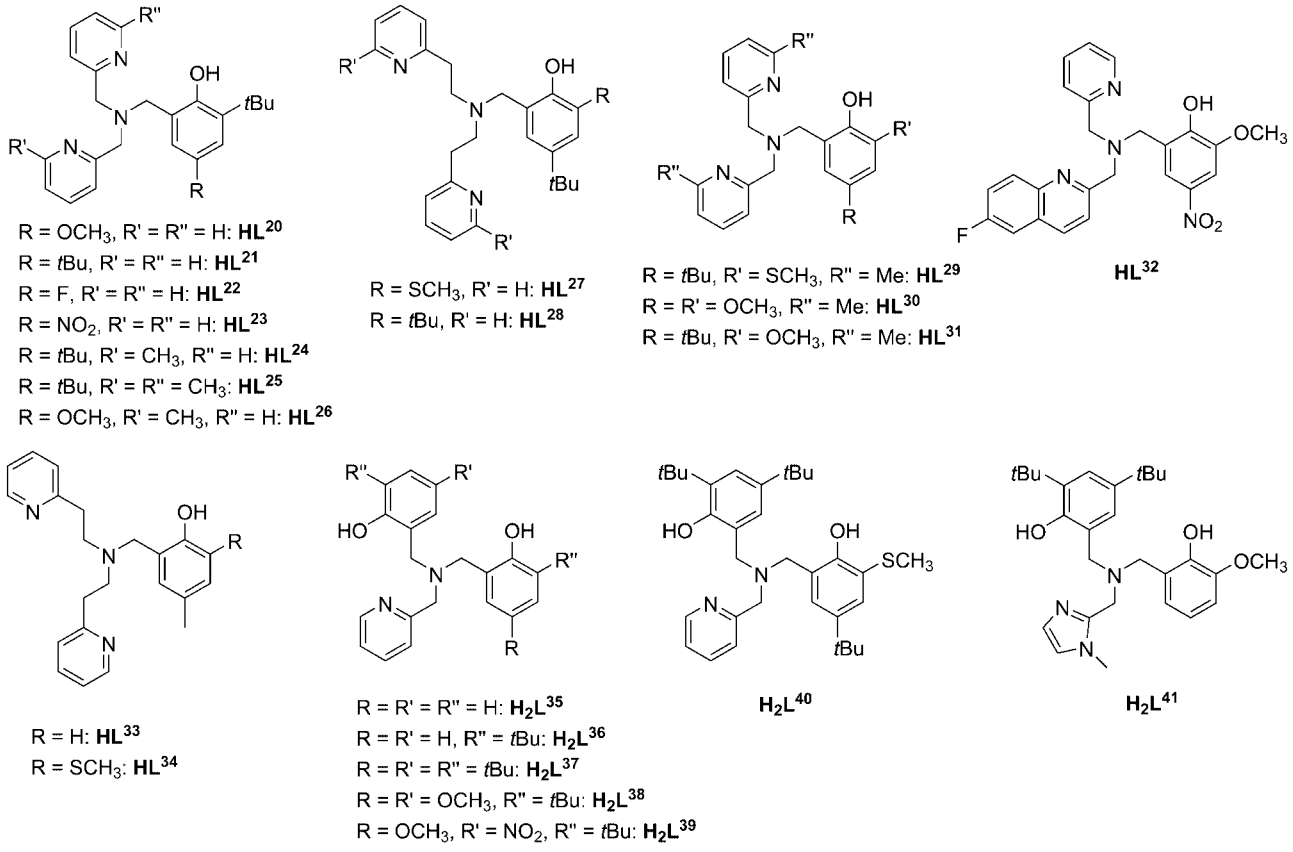

Figure 6. Formulae of some representative tripodal ligands: $HL^{20–23}$ (ref.[58]), $HL^{24,25}$ (ref.[59]), HL^{26} (ref.[60]), $HL^{27,28}$ (ref.[61]), HL^{29} (ref.[62]), $HL^{30,31}$ (ref.[63]), HL^{32} (ref.[64]), $HL^{33,34}$ (ref.[74]), H_2L^{35} (ref.[75]), H_2L^{36} (ref.[65]), H_2L^{37} (ref.[66]), H_2L^{38} (ref.[58]), H_2L^{39} (ref.[58,67]), H_2L^{40} (ref.[68]), H_2L^{41} (ref.[69]).

either in an equatorial[58–61,64,69] or axial[58,71,72] position. The respective influence of the phenolate *para* substituent and alkyl linker arm length on the position of this phenolate have been well documented by Palaniandavar et al. and Fenton et al. (see below). The relative extent of the trigonal-bipyramidal distortion is indicated by the value of τ, which represents the degree of trigonality within the structural continuum between square-planar and trigonal-bipyramidal structures.[70] τ is usually lower than 0.35 for these complexes, which shows that the geometry around the metal ion is predominantly square pyramidal with a slight distortion towards trigonal bipyramidal.[58–61,64,69,71,72] A sample structure is given in Figure 7. In the Cu^{II}-phenolate complexes of $HL^{24,25}$,[59] as well as the Cu^{II}-phenol complexes of HL^{20} and HL^{26},[58,60] the $Cu–N_{methylpyridine}$ bond is longer than the $Cu–N_{pyridine}$ one, which is ascribed to steric hindrance around the methylpyridine nitrogen. All these complexes exhibit a phenolate-to-copper CT transition and less intense d–d transitions as a lower energy tail (λ_{max} > 600 nm, Table 4) in their UV/Vis spectra. λ_{max} of the CT transition is shifted according to the electronic properties of the phenolate substituent (from 565 nm for $[Cu(L^{20})(CH_3CN)]$ to 517 nm for $[Cu(L^{23})(CH_3CN)]$). The EPR spectrum is characterized by a signal that is typical for mononuclear copper(II) species (S = ½; Table 4).

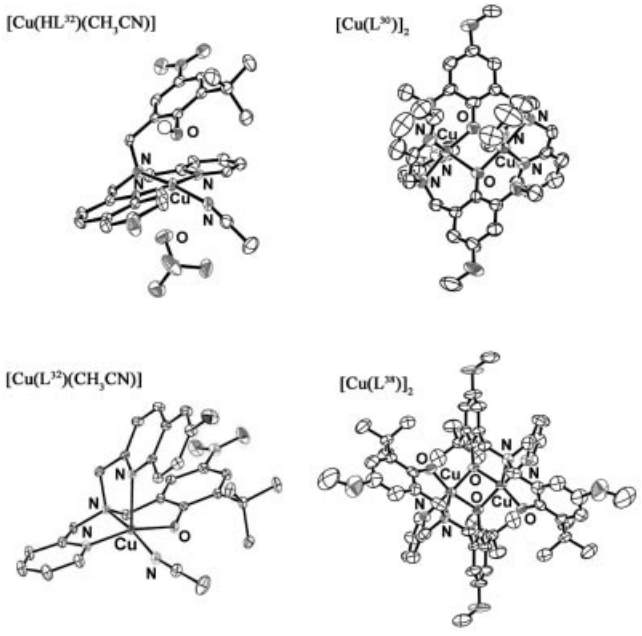

Figure 7. X-ray crystal structures of copper(II) complexes of tripodal ligands $[Cu(HL^{32})(CH_3CN)]$ (ref.[64]), $[Cu(L^{32})(CH_3CN)]$ (ref.[64]), $[Cu(L^{30})]_2$ (ref.[60]), and $[Cu(L^{38})]_2$ (ref.[58]).

Table 4. Properties of some Cu^{II}-phenoxyl radical complexes of tripodal ligands.

Complex	$E_{1/2}$[a]	UV/Vis[b]	Solvent	Ref.
$[Cu(L^{20})(CH_3CN)]$	0.02	565 (1040)	CH_3CN	[58]
$[Cu(L^{20})(py)]$	0.01	546 (950)	CH_3CN	[58]
$[Cu(HL^{20})(CH_3CN)]$	>0.8	400 br. (320), 590 br. (230)	CH_3CN	[58]
$[Cu(L^{21})(CH_3CN)]$	0.15	553 (935), 950 (180)	CH_3CN	[58]
$[Cu(L^{21})(py)]$	0.17	531 (750), 850 (180)	CH_3CN	[58]
$[Cu(HL^{21})(CH_3CN)]$	>0.8	600 (180)	CH_3CN	[58]
$[Cu(L^{22})(CH_3CN)]$	0.20	305 (3400), 535 (920), 930 (130)	CH_3CN	[58]
$[Cu(L^{23})(CH_3CN)]$	0.70	390 (11200), 517 (636)	CH_3CN	[58]
$[Cu(L^{24})(Cl)]$	0.14	519 (1400)	CH_3CN	[59]
$[Cu(L^{25})(Cl)]$	0.19	544 (800)	CH_3CN	[59]
$[Cu(L^{26})(CH_3CN)]$	0.05	564 (870), 660 sh (550)	CH_3CN	[60]
$[Cu(L^{27})]_2$	n.d.	522 (2990)	CH_3CN	[61]
$[Cu(L^{27})(OAc)]$	0.05	473 (880), 660 (220)	CH_3CN	[61]
$[Cu(L^{28})(CH_3CN)]$	0.35	559 (1090)	CH_3CN	[61]
$[Cu(L^{29})]_2$	n.d.	520 (2800)	CH_3CN	[62]
$[Cu(L^{29})(OAc)]$	0.03	490 (970), 690 (240)	CH_3CN	[62]
$[Cu(L^{30})]_2$	0.45	471 (440), 875 (165)	CH_3CN	[63]
$[Cu(L^{30})(py)]$	0.00	556 (560), 900 (310)	CH_3CN	[63]
$[Cu(L^{31})]_2$	0.66	466 (230), 870 (150)	CH_3CN	[63]
$[Cu(L^{31})(py)]$	0.14	530 (640), 900 (250)	CH_3CN	[63]
$[Cu(L^{36})]_2$	0.70 (irr.)	413 (2550), 480 sh, 650 sh, 764 sh	CH_2Cl_2	[65]
$[Cu(L^{36})(CH_3CN)]$	0.11, 0.49 (irr.)	476 (1820)	CH_3CN	[65]
$[Cu(HL^{37})(OAc)]$	0.20	470 (1300)	CH_3CN/CH_2Cl_2	[66]
$[Cu(L^{38})]_2$	–0.14, 0.12	302 (16700), 445 (4330), 650 br. (1600)	CH_2Cl_2	[60]
$[Cu(L^{38})(py)]$	–0.16	310 (20000), 488 (1400)	CH_3CN	[58]
$[Cu(HL^{39})(OAc)]$	0.08	393 (20000), 500 sh (760), 600 br. (510)	CH_3CN/CH_2Cl_2	[58,67]
$[Cu(L^{39})(py)]$	–0.08	305 (6300), 401 (15000), 500 sh (1210), 700 br. (300)	CH_3CN	[58]
$[Cu(L^{40})]_2$	n.d.	453 (2000), 680 (200)	CH_3CN	[68]
$[Cu(L^{40})(py)]$	0.10, 0.33[c]	466 (1360), 710 (100)	CH_3CN	[68]
$[Cu(L^{41})(CH_3CN)]$	–0.07	450 (1000)	CH_3CN	[69]
Complex	**EPR signal[d]**	**UV/Vis[b]**	**Solvent**	**Ref.**
$[Cu(L^{20\cdot})(CH_3CN)]$	$S = 1$	426 (5100), 552 (560)	CH_3CN	[58]
$[Cu(L^{20\cdot})(py)]$	$S = 1$	406 (8200)	CH_3CN	[58]
$[Cu(L^{21\cdot})(CH_3CN)]$	$S = 1$	416 (1900), 650 (500)	CH_3CN	[58]
$[Cu(L^{21\cdot})(py)]$	$S = 1$	417 (3500), 660 (800)	CH_3CN	[58]
$[Cu(L^{22\cdot})(CH_3CN)]$	unstable	unstable	CH_3CN	[58]
$[Cu(L^{23\cdot})(CH_3CN)]$	unstable	unstable	CH_3CN	[58]
$[Cu(L^{24\cdot})(Cl)]$	$S = 1$	418 (3500), 666 (420)	CH_3CN	[59]
$[Cu(L^{25\cdot})(Cl)]$	$S = 1$	406 (2000), 664 (410)	CH_3CN	[59]
$[Cu(L^{26\cdot})(CH_3CN)]$	$S = 1$	427 (3070), 580 (225)	CH_3CN	[60]
$[Cu(L^{27\cdot})(NO_3)]$	silent (77 K)	415 (1790), 867 (550)	CH_3CN	[61]
$[Cu(L^{28\cdot})(NO_3)]$	silent	411 (2440), 675 (300)	CH_3CN	[61]
$[Cu(L^{29\cdot})(CH_3CN)]$	silent (123 K)	424 (1920), 870 (920)	CH_3CN	[62]
$[Cu(L^{30\cdot})(CH_3CN)]$	silent (100 K)	418 (2300), 605 (400)[e]	CH_3CN	[63]
$[Cu(L^{30\cdot})(py)]$	silent (100 K)	420 (6060), 583 (1370)[f]	CH_3CN	[63]
$[Cu(L^{31\cdot})(CH_3CN)]$	nd	420 (3200), 620 (350)[e]	CH_3CN	[63]
$[Cu(L^{31\cdot})(py)]$	silent (100 K)	400 (1125), 687 (300)[f]	CH_3CN	[63]
$[Cu(L^{36\cdot})(CH_3CN)]$	$S = 1/2$	439 (16700), 620 (600)	CH_3CN	[65]
$[Cu(HL^{37\cdot})(OAc)]$	unstable	unstable	CH_3CN/CH_2Cl_2	[66]
$H_2L^{37} + Cu(ClO_4)_2$[g]	silent	403 (2000), 654 (400)	CH_3CN/CH_2Cl_2	[66]
$[Cu(L^{38\cdot})]_2$	silent	416 (3370), 530 (1510), 850 (740)[e]	CH_2Cl_2	[60]
$[Cu(L^{38\cdot})(py)]$	$S = 1$	425 (1000)[f]	CH_3CN	[58]
$[Cu(L^{38\cdot\cdot})(CH_3CN)]$	$S = 1/2$	426 (3600), 650 (540)[e]	CH_3CN	[58]
$[Cu(HL^{39\cdot})(OAc)]$	silent (100 K)	410 (19000)	CH_3CN/CH_2Cl_2	[58,67]
$[Cu(L^{39\cdot})(py)]$	$S = 1$	390 (15300)	CH_3CN	[58]
$[Cu(L^{40\cdot})(py)]$	silent	418 (2100), 720 (100)	CH_3CN	[68]
$[Cu(L^{41\cdot})]_2$	$S = 0$	478 (4500)	CH_3CN	[69]

[a] V vs. Fc^+/Fc. [b] λ [nm] (ε [$M^{-1}cm^{-1}$]). [c] At –40 °C. [d] X-band. The Cu^{II}-phenolate complexes exhibit an $S_{Cu} = ½$ signal except $[Cu(L^{27})]_2$, $[Cu(L^{29–31})]_2$, $[Cu(L^{36})]_2$, $[Cu(L^{38})]_2$ and $[Cu(L^{40})]_2$ (dimeric species). [e] Generated by copper(II) oxidation. [f] Underestimated due to its low stability. [g] Obtained by a disproportionation reaction. No structure reported.

When the complexation reaction is performed with a copper(II) salt that does not contain a strong monoanionic donor and ligands that bear a phenol without steric bulk at its *ortho* position, dimeric species of general formula $[Cu(L^{N_3O})]_2$ are obtained.[61–63,71–75] X-ray structural analysis of $[Cu(L^{30})]_2$ has shown that the two copper ions are

square pyramidal but slightly distorted towards trigonal bipyramidal (Figure 7).[60] The copper ions are bridged by the oxygen atoms of two phenolates, one from each ligand, which can occupy either a mixed axial/equatorial[62,71–73] or exclusively equatorial[62,63,73,74] position in the coordination polyhedron of each copper(II) ion. The two copper ions in these structures are separated by 3.1–3.2 Å and exhibit either an $S = 1$ signal or no signal at all in their EPR spectrum, which indicates that the copper(II) spins interact magnetically (Table 4).[61,62,71–74] The CuOCuO core is almost planar when the phenolate coordinates one copper atom in the axial position, while it shows a slight "butterfly" structure when it coordinates exclusively in the equatorial position.

The copper(II) complexes isolated from N_2O_2 ligands in the presence of NEt_3 are usually dimeric species of general formula $[Cu(L^{N_2O_2})]_2$ irrespective of the bulkiness of the phenolate *o*-substituent.[58,65–67] One example of a mononuclear $[Cu(L^{N_2O_2})(X)]$ structure has been characterized by X-ray diffraction as a biomimetic model of GO,[70] while many others have been obtained by adding coordinating solvents or bases to the $[Cu(L^{N_2O_2})]_2$ dimers.[58,65,75] Even though the chemical formula $[Cu(L^{N_2O_2})]_2$ seems similar to that of $[Cu(L^{N_3O})]_2$, significant differences can be observed between the two. In the $[Cu(L^{N_2O_2})]_2$ dimers, for example, the geometry around the copper(II) ion is more distorted towards trigonal bipyramidal ($\tau = 0.35$ for $[Cu(L^{38})]_2$ shown in Figure 7) and the intermetallic distance is shorter (2.869 Å for $[Cu(L^{38})]_2$). Consequently, the CuOCuO core is not flattened as in $[Cu(L^{N_3O})]_2$ but shows a marked "butterfly" structure (with a dihedral angle of 126° for $[Cu(L^{38})]_2$). The dimers are EPR-silent (Table 4) as a result of a strong antiferromagnetic interaction between the copper(II) ions that we have estimated to be $-189\ cm^{-1}$ for $[Cu(L^{35})]_2$[75] and $-31\ cm^{-1}$ for $[Cu(L^{36})]_2$.[65] The presence of two phenolates per ligand makes the phenolate-to-copper CT transition more intense than in the $[Cu(L^{N_3O})(X)]$ and $[Cu(L^{N_3O})]_2$ complexes (Table 4). We[67] and Fukuzumi et al.[68] have isolated dimeric copper(II) complexes of N_2O_2 ligands possessing two differentiated phenolate arms. In H_2L^{39}, for example, one phenolate bears an electron -withdrawing nitro group while the other possesses an electron-donating methoxy group. We have shown that the electron-donating methoxyl group compensates more efficiently than the nitro group for the electron deficiency on the bridging oxygen atom. The substitution thus orients the position of the phenolate groups in $[Cu(L^{39})]_2$ according to their electronic properties.[67]

In general, conversion of the dimers $[Cu(L^{N_2O_2})]_2$ and $[Cu(L^{N_3O})]_2$ into monomeric structures can be promoted by addition of exogenous donor ligands (pyridine, acetate) or protons.[58,61–63,65,67,68,73–75] In the case of $[Cu(L^{N_3O})]_2$, oxidation (chemical or electrochemical) has also been shown to induce this dimer-to-monomer conversion.[61–63] Dissociation constants can be obtained from spectrophotometric titration of $[Cu(L^{N_3O})]_2$ in the presence of pyridine or acetate. Steric repulsions caused by the 6-methyl groups of the pyridine nucleus significantly lower (one to two orders of magnitude) the stability of the dimers,[62] while an increase in the length of the alkyl linker arm does not significantly affect the dissociation constant.[73,74] The most striking feature is the influence of the phenol *para* substituent: in the presence of pyridine, the dimer $[Cu(L^{33})]_2$ exhibits a dissociation constant 100 times lower than that of $[Cu(L^{34})]_2$. This fact is consistent with an increased steric bulk at the phenolate *ortho* position caused by the methylthio group in $[Cu(L^{34})]_2$ compared to a hydrogen atom in $[Cu(L^{33})]_2$.[74] The coordination sphere has also been found to influence the solution behavior of the dimers. Thus, $[Cu(L^{38})]_2$ remains dimeric in CH_3CN while no such structures could be detected in the solution of the Cu^{II}-phenolate complex of HL^{20}, which suggests a greater stability of the $[Cu(L^{N_2O_2})]_2$ dimer than $[Cu(L^{N_3O})]_2$.[58]

Addition of one molar equivalent of proton [relative to the copper(II) concentration] to the Cu^{II}-phenolate complexes $[Cu(L^{N_2O_2})]_2$, $[Cu(L^{N_3O})]_2$, and $[Cu(L^{N_3O})(X)]$ results in the formation of the corresponding Cu^{II}-phenol complexes $[Cu(HL^{N_2O_2})(X)]$ and $[Cu(HL^{N_3O})(X)]$, as judged by the mononuclear copper(II) signal observed in the final EPR spectrum.[58,63,67,75] The protonation state of these complexes can be confirmed by UV/Vis spectrophotometry as $[Cu(HL^{N_2O_2})(X)]$ and $[Cu(HL^{N_3O})(X)]$ lack the phenolate-to-copper CT transition and only the copper(II) d–d transitions at around 600 nm are observed (Table 4). The copper(II) atom exhibits essentially the same geometry as in the mononuclear Cu^{II}-phenolate complexes, in other words square planar slightly distorted towards trigonal bipyramidal (Figure 7). The X-ray crystal structures of the $[Cu(HL^{20–23})(CH_3CN)]$ complexes (ligand with a N_3O donor set) show that the phenol moiety systematically occupies the more labile axial position in the copper coordination sphere, regardless of the substituent.[58] The axial Cu–O distance is usually longer than 2.4 Å in $[Cu(HL^{20–23})(CH_3CN)]$, while it is around 2.2 Å for axially coordinated phenolates. The phenol group thus only coordinates the copper ion weakly. We have recently shown that deprotonation of the complex $[Cu(HL^{32})(CH_3CN)]$, in which the phenol is *axial*, induces an isomerization (Figure 7):[64] the phenolate moiety coordinates in an *equatorial* position in the deprotonated complex $[Cu(L^{32})(CH_3CN)]$. ^{19}F NMR spectroscopy allowed us to determine a rate constant of $3000 \pm 100\ s^{-1}$ for the following equilibrium at $T = 226$ K:

$$[Cu(HL^{32})(CH_3CN)]^1 + [Cu(L^{32})(CH_3CN)]^2 \rightleftharpoons [Cu(L^{32})(CH_3CN)]^1 + [Cu(HL^{32})(CH_3CN)]^2$$

where superscripts 1 and 2 represent the two distinct complexes that interconvert.

This rate constant is large, thereby indicating that proton transfer and/or molecular rearrangement is extremely rapid.

In the crystal structures of $[Cu(HL^{37})(OAc)]$[64] and $[Cu(HL^{39})(OAc)]$[65] (N_2O_2 ligands) only one phenol is protonated. The ligand in $[Cu(HL^{39})(OAc)]$ possesses two differentiated phenolic arms: since the electron-donating effect of OCH_3 relative to NO_2 makes deprotonation of the hy-

droxyl group more difficult, only that exhibiting the highest pK_a (and thus the lowest oxidation potential) is protonated. This provides evidence for the geometric control of the two different phenolic arms.[67]

The electrochemical behavior of the mononuclear [Cu($L^{20–32}$)(X)] complexes shows an anodic, one-electron redox wave that corresponds to the oxidation of the phenolate moiety to a phenoxyl radical (Figure 8). The oxidation potentials and the chemical stability of the Cu^{II}-phenoxyl radical complexes [Cu($L^{20–23\cdot}$)(X)] are strongly correlated to the σ^+_{Hammet} of the phenolate *p*-substituent ($E_{1/2}$ ranges between 0.01 and 0.70 V vs. Fc^+/Fc, Table 4):[58] The more

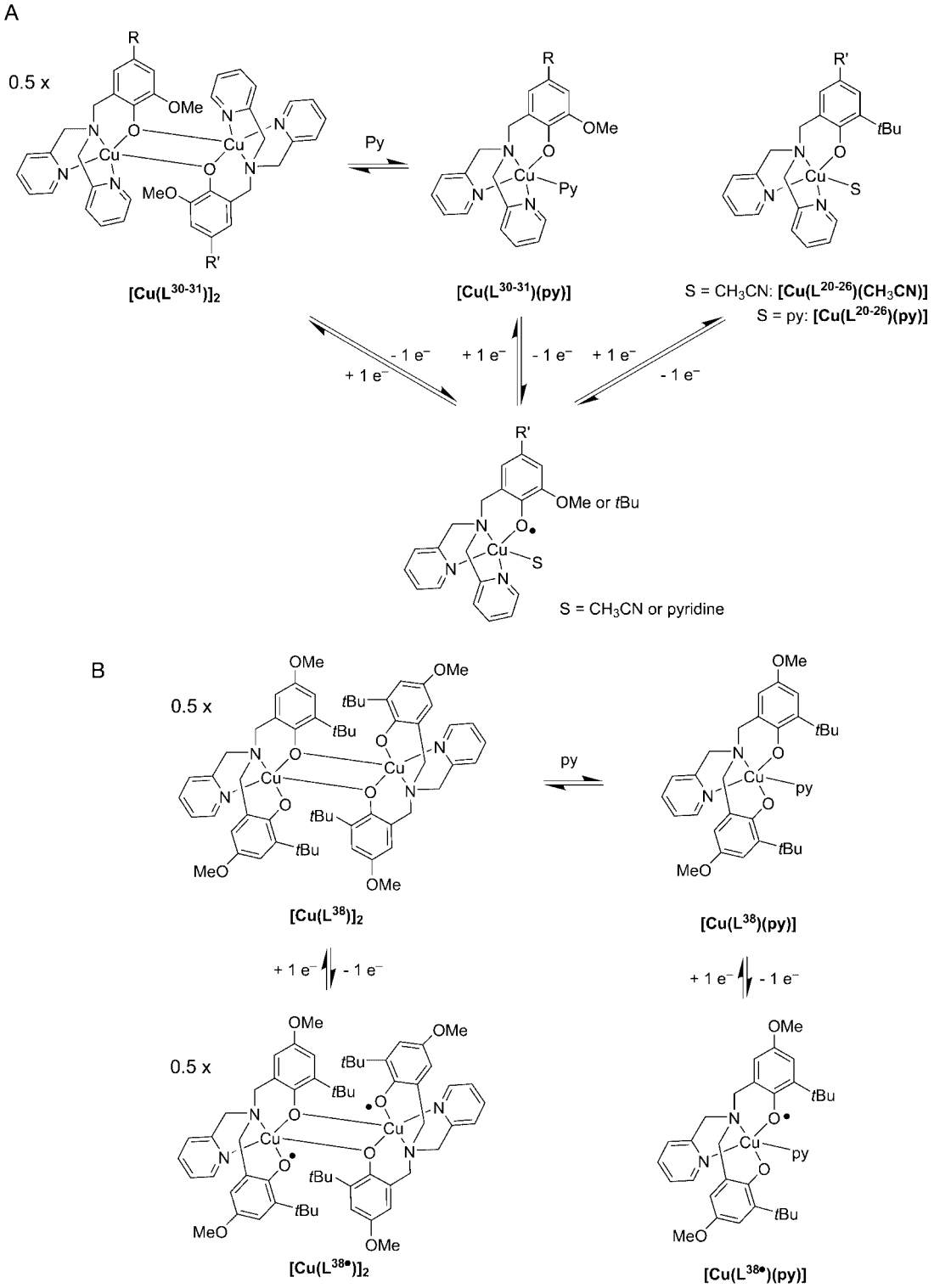

Figure 8. Solution and oxidative chemistry of the copper(II) complexes of $HL^{20–26}$, $HL^{30,31}$, and H_2L^{38}.

electron-donating substituent affords the more stable radical. In addition, a dependence of the radical stability on the N-donor properties has been observed within the $[Cu(L^{24,25})(Cl)]$ and $[Cu(L^{20,26})(CH_3CN)]$ series.[59,60] Thus the weaker N-donor ability of the 2-methylpyridine group compared to pyridine strongly destabilizes the radical complex. The electrochemically (or chemically) generated radical species are either EPR silent or exhibit an $S = 1$ signal (Table 4), thereby showing that the phenoxyl group remains coordinated to the copper(II) ion.[58–64]

The dinuclear species $[Cu(L^{30,31})]_2$ (Figure 8) exhibit an anodic peak, E_p^a, in their CV curves at +0.45 and +0.66 V, respectively, which is associated with a cathodic peak, E_p^c, at much lower potential values (+0.03 and +0.12 V respectively). These E_p^a values are much higher than those of the mononuclear complexes $[Cu(L^{30,31})(py)]$ (py = pyridine; Figure 8, Table 4, $E_{1/2}$ = +0.00 and +0.14 respectively) due to the lower electron density on the bridging phenolate oxygen atom. In addition, the E_p^c values for the dimers are close to those obtained for the monomers $[Cu(L^{30,31})(py)]$. We therefore concluded that the dimers are converted into the monomeric form $[Cu(L^{20–31\cdot})(X)]$ upon oxidation (Figure 8).[63]

Few data concerning the oxidation behavior of the phenolate complexes of N_2O_2 ligands exist.[58,63,65–69,74] The Cu^{II}-phenoxyl complex of HL^{41} has been obtained by treating the ligand with one equivalent of $Cu(ClO_4)_2{\cdot}6H_2O$. A dimeric structure $[Cu(L^{41\cdot})]_2$ with two Cu^{II}-phenoxyl radical molecules bridged by phenolato groups has been proposed for this complex.[69] It is EPR-silent as the result of an antiferromagnetic exchange coupling mediated by the phenolato bridges. We have proposed a similar structure for the radical complex $[Cu(L^{38\cdot})]_2$ (Figure 8).[63] The mononuclear Cu^{II}-phenoxyl complex $[Cu(L^{38\cdot})(py)]$ (Figure 8) was generated by both chemical oxidation and electrolysis[63] and was found to be much less stable than $[Cu(L^{20\cdot})(py)]$, which possesses a similar phenoxyl moiety.[58] This suggests a lower stability of the radical entity formed with $HL^{N_2O_2}$ ligands compared to HL^{N_3O} ligands in spite of their lower oxidation potentials (the difference of oxidation potentials may be at least partially due to the difference of overall charge of the complex). The radical complex $[Cu(L^{36\cdot})(CH_3CN)]$ has been synthesized by chemical oxidation of $[Cu(L^{36})(CH_3CN)]$ with silver acetate.[65] It was found to be EPR-active, which was interpreted as evidence for a weak ferromagnetic or a dipole–dipole interaction between the copper(II) and the axial phenoxyl radical spins. The electrochemically generated $[Cu(HL^{39\cdot})(OAc)]$ species was found to be relatively stable, in agreement with the reversible redox process observed on the electrolysis timescale.[67] Such behavior suggests that no chemical reaction, for example protonation-deprotonation, is associated with the electron transfer, as expected for the oxidation of a protonated phenol.[77] The radical has thus been proposed to be located on the equatorial nitrophenolate group.[67]

The Cu^{II}-phenol complexes $[Cu(HL^{N_3O})(X)]$ exhibit high oxidation potentials (>0.8 V, Table 4) and irreversible cyclic voltammograms,[58,59,63] which can be ascribed to two facts. In uncoordinated phenoxyl radicals, it has been shown that (i) the phenoxonium/phenoxyl redox couple is lower than that for phenoxyl/phenol and (ii) a proton transfer is associated with the electron transfer,[77] which means that the Cu^{II}-phenoxyl radical system cannot be generated from Cu^{II}-phenol complexes. On the other hand, reversible redox waves are observed within the –0.5 to 0.0 V range for these complexes {for example at $E_{1/2}$ = –0.39 V vs. Fc^+/Fc for $[Cu(HL^{21})(Cl)]$}.[59] These waves are attributed to the Cu^{II}/Cu^{I} redox couple. Their relatively high values suggest that the ligand in these Cu^{II}-phenol complexes can efficiently accommodate the copper(I) redox state. In addition, this value is close to that reported for the coordinated phenoxyl/phenolate couple {reversible system at $E_{1/2}$ = +0.02 V vs. Fc^+/Fc for $[Cu(L^{21})(CH_3CN)]$} in the presence of NEt_3.[58] For comparison, the Cu^{II}/Cu^{I} redox potential is –0.24 V in GO vs. Fc^+/Fc, while the tyrosyl/tyrosinate one has been estimated to be –0.01 V vs. Fc^+/Fc at neutral pH.[12,13] The thermodynamic gap between the Cu^{II}/Cu^{I} and phenoxyl/phenolate redox couples of $[Cu(HL^{21})(Cl)]$ and $[Cu(L^{21})(CH_3CN)]$, respectively, is thus close to that measured for GO (0.25 V).

Emerging Classes of Model Compounds for the GO Active Site: Peptide Ligands

A general limitation for the use of chemical analogues of metalloenzyme active sites is their low water-solubility and their poor enantioselectivity when catalyzing reactions. Moreover, structural and reactivity studies on metalloproteins have revealed that the properties of their active sites depend on more than the metal coordination sphere. Modeling the second-sphere interaction in order to improve the biological relevance of complexes mimicking the metalloprotein active sites is therefore a new challenge. An emerging approach that accounts for these factors is the use of oligopeptides as ligands. While the copper(II) coordination chemistry of oligopeptides has been extensively studied, much less is known about the incorporation of biologically relevant radicals in such peptides.

The peptidic approach to modeling the active site of GO has been pioneered by Kojima et al.[78] Their approach concerns the use of cyclic tripeptides such as Boc-Gly-e(His-Tyr-OEt) (e is an ethylene bridge) that incorporate both a tyrosine and a histidine ligand for the copper ion. A 2:1 ligand:metal complex is predominantly formed in solution whose structure involves a square-pyramidal monomer complex coordinated to two imidazole nitrogens atoms, two phenolate oxygen atoms, and one external water or solvent molecule. Its electrochemical behavior shows an irreversible ligand-centered oxidation process at +0.91 V vs. Fc^+/Fc attributed to the phenoxyl/phenolate redox couple. This value is much higher than that of GO, which shows that the radical is not stable.

Five years later, two reports by Berkessel[79] and ourselves[80] appeared in the literature, both of which concern the synthesis of peptides designed to stabilize phenoxyl rad-

icals generated on their side chains. Berkessel et al. used a strategy based on combinatorial synthesis using peptide chemistry.[79] The general design of the solid-phase-bound decapeptide library is shown in Figure 9. A Pro-Gly sequence is included in order to induce a hairpin that makes the X_1–X_4 residues orient properly to chelate a copper(II) ion. These four positions (X_1–X_4) are occupied in a combinatorial manner by histidine, tyrosine, modified cysteine (cross-linked with a di-*tert*-phenol moieties), or a modified TEMPO (stable nitroxide radical). Incubation of the solid-phase-bound library with copper results in a color change, which indicates metal binding. The His-rich sequences gave blue beads, Tyr-rich sequences pale yellow to green complexes, while the presence of the modified TEMPO in the peptide resulted in an orange coloration. The solid-phase-bound peptide libraries were screened for their activity towards benzyl alcohol and 3-methoxybenzyl alcohol oxidation. A pronounced sequence-dependence of the catalytic activity was observed: the most active ligands were those incorporating the modified TEMPO group, which allow up to six turnovers. No deactivation of the catalyst due to oxidative demetalation was observed, and characterization of the (radical) copper complexes is currently in progress.

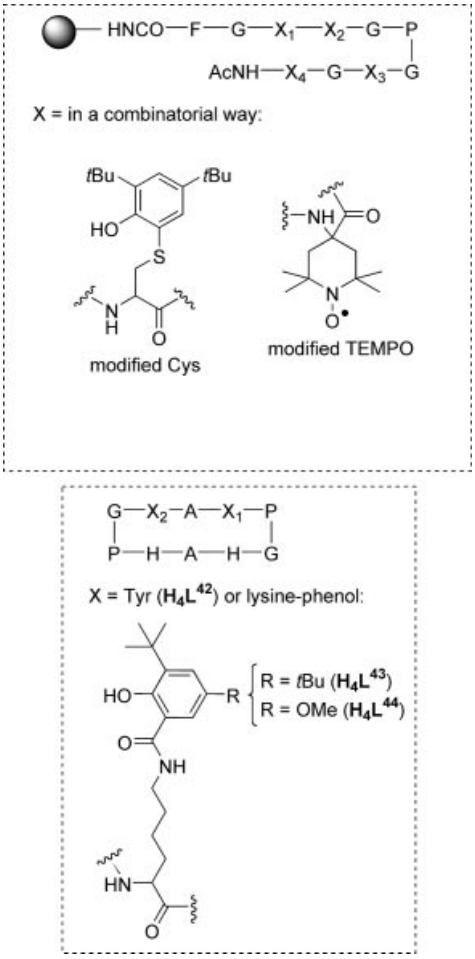

Figure 9. Formulae of peptide ligands. The top structure is adapted from ref.[79] and the bottom one from ref.[80]

In another approach, we have used cyclic decapeptides incorporating two proline-glycine sequences to induce β-turn hairpins.[80] The resulting peptide conformation is constrained into an anti-parallel β sheet and functionalization is achieved above the plane of this motif by two histidines and two amino acids X_1 and X_2 [X_1 and X_2 being either tyrosines (H_4L^{42}) or a lysine-phenol conjugate ($H_4L^{43,44}$)]. Potentiometric titrations have shown that deprotonation of the phenol moieties requires a pH higher than 12 (the corresponding pK_a values range between 8.96 and 11.34, depending on the amino acid X). At pH 12.2 only the decapeptides incorporating a lysine-phenol conjugate exhibit reversible signals [$E_{1/2}$ = –0.03 V for R = *t*Bu (L^{43}) and –0.20 V vs. Fc^+/Fc for R = OMe (L^{44})], thereby showing that the stability of the oxidized species is noteworthy. This stability is confirmed by electrochemical oxidation of the peptides, which affords EPR-active species whose spectra are typical of phenoxyl radicals. These compounds are among the first radical-peptides to be generated and persist in solution long enough to be characterized. Evaluation of their coordination chemistry is currently in progress.

Emerging Classes of Model Compounds for the GO Active Site: Calix[6]arene Ligands

Another platform, namely calix[6]arenes, has been pioneered by Reinaud et al.[81] In these systems, a four- or five-coordinate metal ion is constrained in a mononuclear environment that preserves a binding site buried inside a hydrophobic pocket accessible to small molecules. In order to get model compounds for the GO active site, the calix[6]arene core has been functionalized with one phenol and three *N*-methylimidazole groups. In the copper(II) complex, the metal ion is pentacoordinate and has a square-pyramidal geometry. The phenolate oxygen and one solvent molecule (acetonitrile) bind in equatorial positions, while the three *N*-methylimidazole nitrogens complete the pyramid. The solvent is buried in the conic cavity of the calixarene in a *trans* position relative to the phenolate group, which caps the copper(II) complex. The Cu^{II}-phenoxyl radical complex was found to be able to mediate the stoichiometric two-electron oxidation of benzyl alcohol. This reaction is promoted by coordination to the copper and proceeds in an inner-cavity process.

Modeling the Properties of the GO Active Site

Influence of the Cys-Tyr Crosslink

In order to better understand the influence of the Cys-Tyr crosslink on the properties of the redox-active Tyr272 residue of the enzyme, Itoh et al. have synthesized a series of 2-methylsulfanylphenols.[74] These compounds exhibit oxidation potentials that are much lower than those of the nonsubstituted parent phenols, with, for example, a drop of 0.35 V on going from the 4-methylphenol to the 4-methyl-2-methylsulfanylphenol. Such behavior is interpreted in

terms of the electron-sharing conjugative effect of the methylsulfanyl substituent.

The corresponding phenoxyl radicals have been generated by pulse radiolysis. The 4-methylphenoxyl radical species exhibits two intense absorptions in its UV/Vis spectrum at around 400 nm corresponding to π–π* transitions. The UV/Vis spectrum of the 4-methyl-2-methylsulfanylphenoxyl radical also shows such absorptions at around 400 nm, but exhibits an additional strong absorption band at 850 nm. The origin of this latter absorption has been attributed to an intramolecular charge transfer from the benzene ring to the methylsulfanyl group. It is important to note that this lower-energy feature is quite similar to that of the enzyme in its radical form. It has been proposed that the larger ε value obtained for GO arises from an interligand charge transfer from the Tyr272 radical to Tyr495.[82] EPR spectroscopy has revealed that a methylsulfanyl substituent induces larger *g*-tensor values for the phenoxyl radical due to the large spin-orbit coupling on the sulfur atom (g = 2.0060 for the 4-methyl-2-methylsulfanylphenoxyl radical; g = 2.0036 for the 2,4,6-trimethylphenoxyl radical).[74] A large amount of spin density thus delocalizes over the sulfur atom of the methylsulfanyl substituent.

Some copper(II) complexes bearing coordinated 2-(alkylsulfanyl)phenoxyl radical derivatives have been synthesized (Figure 10).[34,61,62,83,84] The complex [Cu(L^{45})(ppb)], for example, which is obtained by treating one equivalent of 2-hydroxy-5-methyl-3-(methylsulfanyl)benzaldehyde with one equivalent of tris(3-phenylpyrazolyl)borate (ppb) and copper(II), can be oxidized into a radical species. The 2-alkylsulfanylphenol moiety has also been incorporated into Schiff bases (H_2L^2)[34] and tripodal ligands ($HL^{27,28}$, H_2L^{40})[61–68] and the corresponding mononuclear Cu^{II}-phenoxyl complexes characterized. The UV/Vis spectra of all the non-Schiff base species typically exhibit both the strong absorption bands at around 400 nm and the NIR feature above 800 nm that were observed in the 2-(methylsulfanyl)-phenols. In the Schiff-base series, the anticipated phenoxyl radical absorption feature at 400 nm is obscured by intense ligand absorption bands. All the Cu^{II}-phenoxyl species were found to be X-band EPR-silent as a result of a magnetic coupling between the copper(II) and the radical spins.

It has previously been proposed by Stack et al. that salen complexes fail to reproduce the high turnovers of GO because of their inability to form stable copper(I) complexes.[34,35] A pentadentate NO_2S_2 ligand (H_2L^{46}) that incorporates *ortho*-(alkylsulfanyl)phenol moieties has therefore been prepared.[85] A major difference between this ligand and most of the previous ones is that the sulfanyl groups here are designed to coordinate the copper atom, which is expected to both lower the phenol oxidation potential and increase the redox potential of the Cu^{II}/Cu^{I} couple. Unfortunately, the X-ray crystal structure of its copper(II) complex [Cu(L^{46})] shows that the occupied electron-donating sulfur p orbitals are aligned to bond to the copper center rather than π-conjugated with the phenolates, and that the copper(II)–sulfur bonds are long (>2.4 Å). Its high oxidation potentials (+0.47 and +0.62 V vs. Fc^+/Fc) confirm

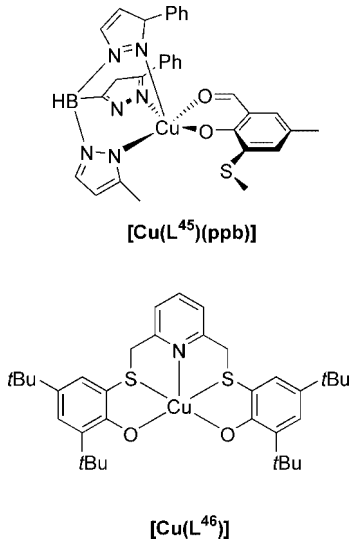

Figure 10. Copper(II) complexes of ligands possessing a 2-(alkylsulfanyl)phenoxyl moiety: [Cu(L^{45})(ppb)] (ref.[83]) and [Cu(L^{46})] (ref.[85]).

that the sulfur groups behave as electron-withdrawing groups. The reduction wave, which is attributed to the Cu^{II}/Cu^{I} couple, is observed at –1.23 V, close to the value reported for binaphthyl-salen complexes such as [Cu(L^2)]; all attempts to isolate the copper(I) complex were unsuccessful.

Modelling the Tyr-Trp π–π Interaction

The X-ray crystal structure of the GO active site has revealed that the redox-active tyrosine is π-stacked with the indole ring of a neighboring tryptophan Trp290 residue. This interaction has been modeled in several ways by Halcrow et al.[86–90] In one approach, they synthesized 3,4-benzo-8,9-(3′-hydroxy-4′-methylsulfanylbenzo)bicyclo-[4.4.1]undeca-3,8-dien-11-one (HL^{47}) and its ethylene acetal HL^{48} (Figure 11).[86,87] The ketone adopts a boat/chair conformation while the acetal exhibits a chair/chair conformation with layered benzo rings. The oxidation potential, which is 0.15 V lower for HL^{48} than for HL^{47}, may suggest that the π–π interaction contributes to the thermodynamic stability of the oxidized species, although an alternative explanation is that the identity of the bridgehead group (ketone vs. acetal) has an effect on the p-orbital energy. As this suggestion has not yet been quantified, the authors still entertain both possibilities. The cyclic voltammograms also revealed an improved reversibility for HL^{47}, which could be attributed to both an intramolecular O–H···S hydrogen bond that would hinder deprotonation of the oxidation product and steric protection afforded by the intramolecular π–π interaction.

In another approach, they have synthesized the ligand L^{49}, which contains an oxidizable dimethoxyphenyl substituent.[88–90] In its copper(II) complexes [Cu(L^{49})(TpPh)] and [Cu(L^{49})(TpCy)] {Tp = tris(3-arylpyrazolyl)hydroborate; TpPh: R = phenyl, TpCy: R = cyclohexyl} the metal ion

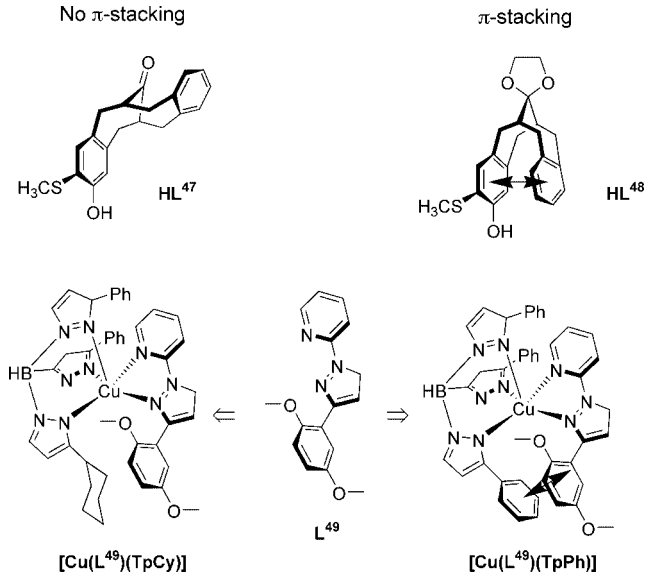

Figure 11. Model compounds for the Tyr-Trp π–π interaction: HL^{47} and HL^{48} (ref.[86,87]), $[Cu(L^{49})(TpCy)]$ and $[Cu(L^{49})(TpPh)]$ (ref.[88–90]).

resides within the same square-pyramidal geometry. Nevertheless, a major difference exists between each complex: The dimethoxyphenyl group in $[Cu(L^{49})(TpPh)]$ takes part in a π–π interaction with a phenyl ring from the TpPh coligand while no such interaction exists within $[Cu(L^{49})(TpCy)]$. The authors have shown that the π–π interaction exhibited by $[Cu(L^{49})(TpPh)]$ is retained following its one-electron oxidation, although deconvolution of the voltammograms led to the conclusion that this interaction has no measurable effect on the kinetic stability of the resultant aryl radical.

Recently, we have suggested a structural role for this interaction:[64] The metal in $[Cu(HL^{32})(CH_3CN)]$ has a square-pyramidal geometry whose apical position is occupied by the phenol moiety. In the deprotonated complex $[Cu(L^{32})(CH_3CN)]$, this phenolate group has shifted to an equatorial position, which means that an isomerization is induced by deprotonation. π–π stacking interactions between the phenolate and quinoline rings that have been detected in the solid state are proposed to contribute, at least partially, to the isomerization and thus the phenolate positioning.

In summary, the Tyr-Trp π–π interaction in GO is supposed to have little or no effect on the chemical reactivity of the tyrosyl radical, except to shield it from external solvent. All these biomimetic studies thus suggest that the role of this interaction in GO is structural rather than electronic – it has been proposed recently that it may be involved in maintaining the cofactor orientation that results in the diamagnetic ground state of GO.[17]

Understanding the Diamagnetic Ground State of the Oxidized Form of GO

GO is EPR-silent in its copper(II)-tyrosyl radical form as the result of an antiferromagnetic coupling between the radical and the Cu^{II} spins.[16] The relative orientations of the magnetic orbitals of the Cu^{II} ion ($d_{x^2-y^2}$) and of the phenoxyl radical (half-occupied π orbital) are expected to determine the multiplicity of the electronic ground state (Figure 12). Quantification of this orientation can be roughly achieved by measuring the Cu^{II}–O–C bond angle (α) and the dihedral angle (β) between the x,y plane at the Cu^{II} ion and the phenyl ring of the radical ligand in the X-ray crystal structures of Cu^{II}-phenolate complexes (Figure 12). Wieghardt et al. have been able to tune these angles, and thus the multiplicity of the electronic ground state, in a series of copper(II) complexes of TACN ligands.[52] Increasing the coordination number from five to six does not change α significantly {125.2° in $[Cu(L^{15})(Cl)]$ vs. 129.2° in

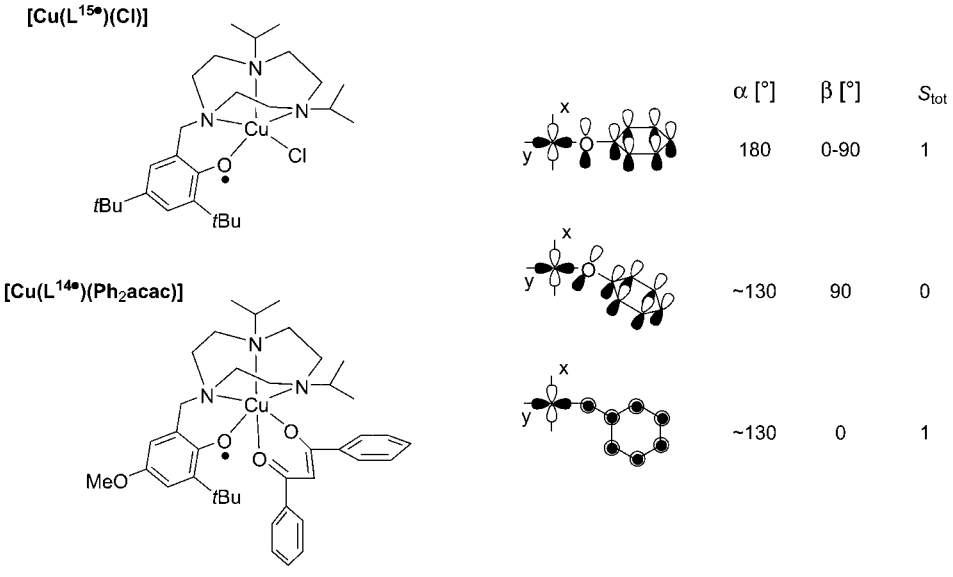

Figure 12. Models for the multiplicity of the ground state of GO (adapted from ref.[52]).

[$Cu(L^{14})(Ph_2acac)$]}, whereas β decreases by nearly 10° {27.4° in [$Cu(L^{15})(Cl)$] vs. 17.6° in [$Cu(L^{14})(Ph_2acac)$]}. These structural changes induce the inversion of the sign of the magnetic coupling, from antiferromagnetic in [$Cu(L^{15\cdot})(Cl)$] to ferromagnetic in [$Cu(L^{14\cdot})(Ph_2acac)$] ($J = 16 \pm 3$ cm^{-1} for the latter complex). In GO, the bond angles α and β are about 129° and 75°, respectively, consistent with an antiferromagnetic coupling, as in [$Cu(L^{15\cdot})(Cl)$].[12,13,52]

Structural Approaches to the GO Active Site [Axial Copper(II)-Tyrosinate Bond and Coordinated Phenoxyl Radical]

One of the first biomimetic approaches to the GO active site involved modeling the axial copper(II)-tyrosinate bond. Three groups have reported X-ray crystal structures of copper(II) complexes involving unusually axially coordinated phenolates as model compounds for GO.[58,71,72,91–93] The ligands used in these studies possess a tripodal structure with a pendent phenol arm that is substituted at its *para* position by an electron-withdrawing nitro group. In the copper(II) complex [$Cu(L^{50})(Cl)$] (Figure 13), the geometry around the metal center is square pyramidal, with two pyridine nitrogens, one tertiary amine nitrogen, and an exogenous ligand (chloride ion) in the basal plane. The phenolate oxygen binds weakly in the *apical* position, thus making this complex the first that reproduces the axial Cu^{II}-phenolate bond of GO.[94] It was initially proposed that the apical coordination of the phenolate is due to the introduction of the nitro substituent *para* to the phenolate group, as in its absence phenolates occupy the equatorial position.[91] The polarity rule, which states that the more electronegative ligand will preferentially occupy the axial position of a tetragonal-based pyramid, was proposed to account for these results in combination with crystal-packing forces. Lately, Fenton et al. have published the X-ray crystal structure of the copper(II) complex of HL^{51} (Figure 13),[71,92] in which the nitrophenolate occupies the *equatorial* position. These contradictory results can be rationalized by considering the size of the chelate rings, since a five/five/six-membered chelate ring sequence is observed in Palaniandavar's complexes whereas a six/six/six-membered chelate ring sequence is observed in Fenton's complex. We have structurally characterized the Cu^{II}-phenolate complexes of HL^{23} and HL^{32}.[58,64] Both ligands possess similar 2-*tert*-butyl-4-nitrophenol and pyridine moieties but differ in their third chelating arm (a pyridyl group for HL^{23} and a fluoroquinolyl group for HL^{32}). The nitrophenolate moiety in [$Cu(L^{23})(Cl)$] is found to coordinate in an axial position while in [$Cu(L^{32})(CH_3CN)$] it occupies the equatorial position. Formation of an axial phenolate oxygen–copper bond thus appears not only related to the electronic properties of the phenolate *para* substituent but also to steric factors arising from the ligand and to the nature of the chelate rings formed.

To duplicate and better understand the anion interactions in the inactive enzyme and the spectral changes ac-

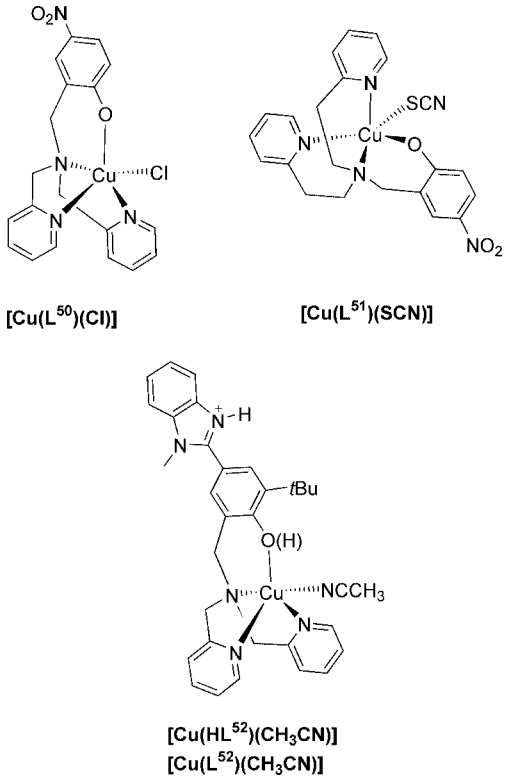

Figure 13. Models for the axial copper-phenolate bond: [$Cu(L^{50})(Cl)$] (ref.[91]), [$Cu(L^{51})(SCN)$] (ref.[92]), [$Cu(HL^{52})(CH_3CN)$] and [$Cu(L^{52})(CH_3CN)$] (ref.[93]).

companying it,)Palaniandavar et al. have determined the crystal structures of a series of [$Cu(L^{50})(X)$] complexes (X = ClO_4^-, SCN^-, $CH_3CO_2^-$).[72] Replacement of a weakly coordinating ligand X by a strongly coordinating one in the equatorial position has been shown to decrease the electronic interaction between the metal center and the axially coordinated phenolate, and consequently contributes to a lengthening of the axial Cu–O bond [2.186(2), 2.200(3), and 2.268(1) Å for X = SCN^-, $XCH_3CO_2^-$ and Cl^-, respectively].

With the aim of visualizing the effect of protonation of the axial phenolate on the metal–ligand bonds, we have synthesized the Cu^{II}-phenol and Cu^{II}-phenolate complexes of HL^{23}.[58] The phenolate complex [$Cu(L^{23})(Cl)$] exhibits a geometry that is roughly similar to that of [$Cu(L^{50})(Cl)$] described by Palaniandavar et al.[94] We also reported the X-ray crystal structures of the phenol complex [$Cu(HL^{23})(CH_3CN)$], but as the exogenous ligand is different in the phenolate and phenol structures (an acetonitrile molecule in the former and a chloride ion in the latter) it was difficult to estimate the influence of the protonation of the axial phenolate on the equatorial bonds. We therefore synthesized the copper(II) complex of HL^{52}, which bears an electron-withdrawing *N*-methylbenzimidazolium instead of a nitro substituent.[93] The phenolate and phenol complexes could be crystallized with the same exogenous ligand (acetonitrile molecule). From the X-ray structure analysis, it appears clear that deprotonation of the axial phenol forces the metal to move out of the basal plane towards the oxygen atom (as a consequence of a stronger axial bond),

and that both $Cu–N_{pyridine}$ bond lengths increase, thereby reflecting the weakening of the equatorial bonds (Figure 14). Interestingly, the phenolate compound $[Cu(L^{52})(CH_3CN)]$ exhibits the shortest axial $Cu–O_{phenolate}$ distance in the whole series of complexes [2.133(4) Å].

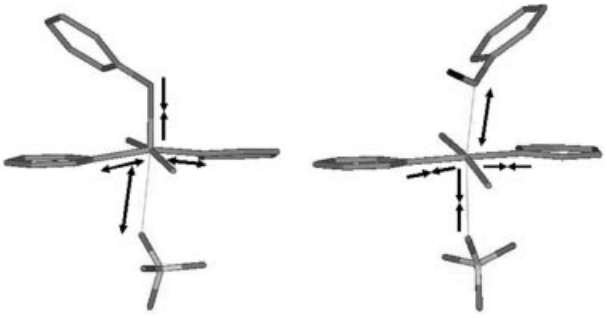

Figure 14. Effect of the protonation of the phenolate moiety on the bond lengths around the copper atom (reproduced from ref.[93]).

Several X-ray crystal structures of transition metal complexes of ligands possessing iminosemiquinonate moieties have been reported.[45,95] The first X-ray crystal structure of coordinated phenoxyl radical was reported in 1996 by Wieghardt et al.[96] for a phenoxylchromium complex. The crystal structure of a copper(II)-coordinated phenoxyl radical was obtained in 2001.[97,98] The complex $[Cu(L^{53})_2]$ has been structurally characterized (Figure 15) and chemically oxidized to $[Cu(L^{53\cdot})(L^{53})]$. The two ligands in $[Cu(L^{53\cdot})(L^{53})]$ are structurally inequivalent (Figure 15): one (L^{53}) exhibits C–C, C–O, and C–N bond lengths that are similar to those of $[Cu(L^{53})_2]$, whereas in the second ($L^{53\cdot}$) the phenol C–O distance is significantly shorter and the two adjacent C–C bonds and the Cu–O bond are longer than those in $[Cu(L^{53})_2]$. The C–O distance of 1.264(5) Å reported for $L^{53\cdot}$ emphasizes the C=O character of this bond [it is 1.322(5) Å in L^{53}]. The other metal–ligand bonds in $[Cu(L^{53\cdot})(L^{53})]$ are significantly shorter than in $[Cu(L^{53})_2]$. All these C–O and C–C bond lengths are in agreement with the electronic structure depicted in Figure 15, where the unpaired electron of the phenoxyl group is delocalized over both *ortho* positions.

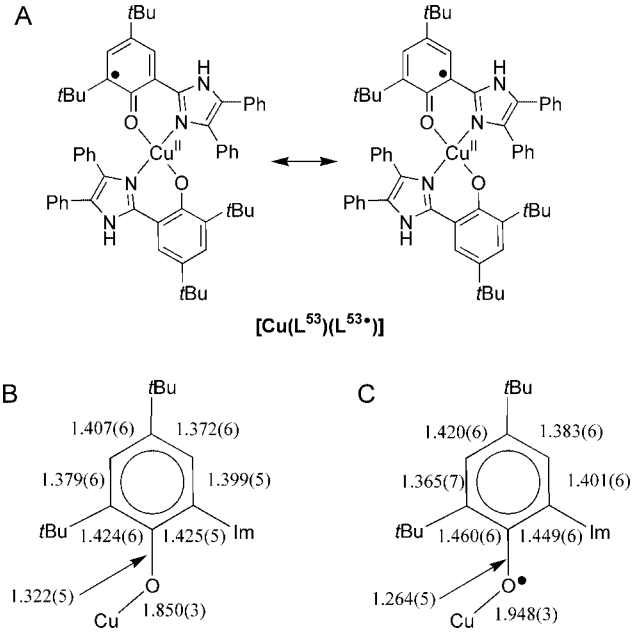

Figure 15. Formula of $[Cu(L^{53})(L^{53\cdot})]$ and its resonance structures (A) and bond lengths of the phenolate moiety (B) and phenoxyl radical moiety (C) coordinated to the copper(II) ion of $[Cu(L^{53})(L^{53\cdot})]$ (adapted from ref.[97]).

Reactivity of Copper(I) Complexes Towards O_2

The catalytic reaction for GO occurs via a ping-pong mechanism.[9–11] The first half-reaction involves binding and oxidation of the alcohol substrate by the Cu^{II}-tyrosyl radical form to yield aldehyde and the reduced copper(I) state. In the second half-reaction dioxygen is bound and reduced, releasing H_2O_2 and the Cu^{II}-tyrosyl radical form of the enzyme. The first step has been studied extensively, while very little is known about the dioxygen reactivation step. It has been speculated that O_2 binds to the three-coordinate copper(I) site to form a Cu^{II}-superoxide species, which evolves into a Cu^{II}-hydroperoxide-tyrosyl radical intermediate. A proton transfer from the axial tyrosine leads to the release of H_2O_2 and regeneration of the initial Cu^{II}-tyrosyl radical form of the enzyme. With the goal of obtaining insights into the dioxygen reactivation step, Tolman et al. have characterized Cu^{I}-phenolate complexes and studied their reactivity towards O_2 by low-temperature stopped-flow experiments.[55] They have shown that the copper(I) phenolate complex $[Cu^{I}(L^{15})]$ has a four-coordi-

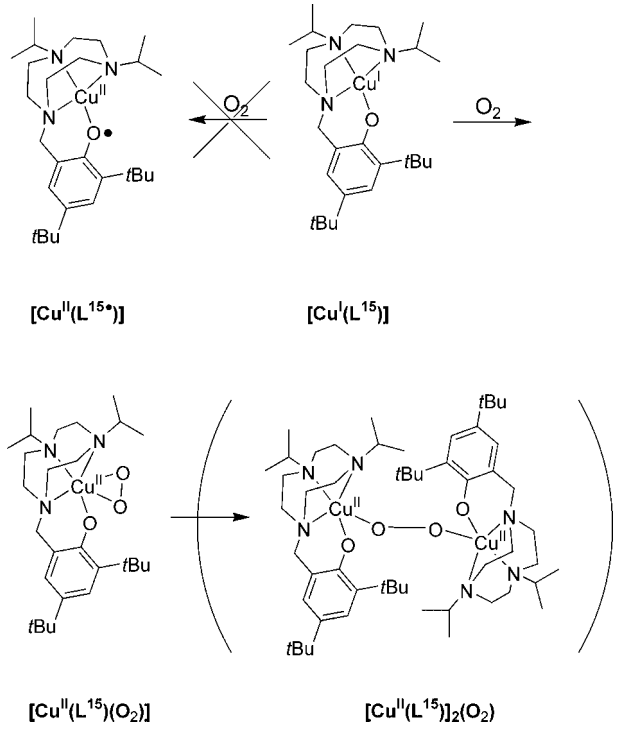

Figure 16. Reactivity of TACN complexes with O_2 (ref.[55]).

nate geometry (Figure 16) while $[Cu^{I}(L^{16})]$ adopts a planar three-coordinate geometry. The average metal–ligand bond lengths are 2.13 Å in $[Cu^{I}(L^{15})]$ and 2.05 Å in $[Cu^{I}(L^{16})]$. The former fits much better with the value of 1.99 Å determined from EXAFS measurements in the enzyme, thereby suggesting that a coordination number of about three is more appropriate for the enzyme. $[Cu^{I}(L^{16})]$ was found to be too reactive with O_2 even at cryogenic temperatures, thus precluding a detailed investigation. Mixing $[Cu^{I}(L^{15})]$ with excess O_2 produced dark-green solutions, while sub-stoichiometric amounts of O_2 afforded a green solution that reacted rapidly to form an intensely purple species.

This was interpreted in terms of the following reaction sequence (see also Figure 16).

$[Cu^{I}(L^{15})] + O_2 \rightleftharpoons [Cu^{II}(L^{15})(O_2)]$ "green species"

$[Cu^{II}(L^{15})(O_2)] + [Cu^{I}(L^{15})] \rightarrow [Cu^{II}(L^{15})]_2(O_2)$ "purple species"

$2 \times [Cu^{II}(L^{15})(O_2)] \rightarrow [Cu^{II}(L^{15})]_2(O_2) + O_2$ "purple species"

$[Cu^{II}(L^{15})]_2(O_2) \rightarrow$ decomposition

The dark-green species $[Cu^{II}(L^{15})(O_2)]$ exhibits λ_{max} values at 416 (ε = 4600) and 654 nm (1800 $M^{-1}cm^{-1}$), which are slightly different than those of the corresponding and fully characterized Cu^{II}-phenoxyl radical species $[Cu^{II}(L^{15\cdot})(CH_3CN)]$ [λ_{max} = 410 (ε = 4000) and 672 nm (1000 $M^{-1}cm^{-1}$); Table 3].[54] The Raman spectrum of $[Cu^{II}(L^{15})(O_2)]$ is characterized by a peak at 1120 cm^{-1}, for the $^{16}O_2$ sample, which shifts to 1058 cm^{-1} when $^{18}O_2$ is used. Based on comparison with literature data, this could be attributed to the ν(O–O) mode of a superoxidocopper(II) complex (Figure 16). With mixed isotopically labeled gas an additional sharp peak was observed at 1093 cm^{-1}, without splitting, which suggests a symmetric (η^2) binding of the superoxide ligand (Figure 16). The ν(Cu–O_2) mode was observed at 422 and 450 cm^{-1}, while additional features not sensitive to $^{18}O_2$ substitution, corresponding to a phenolate mode, are observed at approximately 1300 cm^{-1} and in the region 1500–1700 cm^{-1}. This species is EPR-silent as the result of a magnetic coupling between the copper(II) and the superoxide ligand.

The purple species $[Cu^{II}(L^{15})]_2(O_2)$, which exhibits multiple broad bands that are sensitive to ^{18}O-isotope substitution in the regions 500–550 and 700–850 cm^{-1}, could be described as a peroxidodicopper complex (Figure 16). The unusual broadening of these signals is attributed to the existence of multiple conformational isomers that differ with respect to the metal ion geometry and/or the relative ligand donor disposition (Figure 15).

The peroxido species $[Cu^{II}(L^{15})]_2(O_2)$ prevails at all temperatures while the superoxido one $[Cu^{II}(L^{15})(O_2)]$ cannot be observed unless $[Cu^{I}(L^{15})]$ is present in excess. In contrast, in most previously described systems the peroxido compound is the stable species in the presence of excess O_2 while the superoxido complex is no more than an intermediate. Such a difference may result from the presence of a phenolate (and its electronic effect) or steric bulk provided by the *i*Pr and *t*Bu substituents in HL^{15}. The light-green decomposition products are probably multinuclear copper(II)-containing species, although their exact nature is unknown.

We have studied the reactivity of copper(I) complexes of tripodal ligands that are precursors of stable phenoxyl radicals with O_2.[63] The copper(I) complexes were generated in situ and oxygenation was performed at 233 K. We have shown in the case of the copper(I) complex of the N_3O ligands HL^{20} and HL^{30} that O_2 does not oxidize the phenol into a phenoxyl radical. Instead, a Cu^{II}-phenolate complex is obtained. In contrast, reaction of O_2 with the copper(I) complex of the N_2O_2 ligand H_2L^{38} affords products whose spectral properties are quite different to those of isolated Cu^{II}-phenolate and Cu^{II}-phenoxyl species. A highly reactive transient species is then formed and decomposes in solution, although its nature remains unclear.

Radical Cofactor Formation: Reactivity of Tripodal Ligands Towards Cu^{2+}

It has recently been shown that formation of the radical cofactor of GO can be achieved by treating copper and O_2 with the pre-form of GO.[29,30] With the aim of better understanding the way in which copper(II) might be involved in GO activation, we have studied the reactivity of several tripodal ligands at various copper(II) [added as its $Cu(ClO_4)_2{\cdot}6H_2O$ salt], base, and dioxygen concentrations in CH_3CN.[63] Addition of 0–1 molar equivalents of Cu^{2+} to the phenolate complex $[Cu(L^{20})(CH_3CN)]$ (ligand possessing a N_3O donor set) or 1–2 molar equivalents of Cu^{2+} to the ligand HL^{20} in the presence of NEt_3 results in dramatic color changes. No more changes were observed beyond two molar equivalents of added copper(II). UV/Vis, EPR, and electrochemical characterizations indicated that the reaction product was the Cu^{II}-phenoxyl radical complex $[Cu(L^{20\cdot})(CH_3CN)]$, which is quantitatively formed by chemical oxidation of $[Cu(L^{20})(CH_3CN)]$ by excess solvated Cu^{2+} according to:

$$[Cu(L^{20})(CH_3CN)] + Cu^{2+} \rightarrow [Cu(L^{20\cdot})(CH_3CN)] + Cu^{+}$$

A reverse titration, in other words addition of HL^{20} to Cu^{2+} in the presence of NEt_3, showed that half an equivalent of $[Cu(L^{20\cdot})(CH_3CN)]$ is formed at a HL^{20}/Cu^{2+} ratio of 0.5, the remaining copper being in the Cu^{+} redox state. At one molar equivalent of added ligand, $[Cu(L^{20})(CH_3CN)]$ is formed quantitatively in a comproportionation reaction.

$$\mathbf{[Cu(L^{20\cdot})(CH_3CN)]} + Cu^{+} + \mathbf{HL^{20}} \xrightarrow{NEt_3} \mathbf{2\,[Cu(L^{20})(CH_3CN)]}$$

Addition of one molar equivalent of Cu^{2+} to the phenol complex $[Cu(HL^{20})(CH_3CN)]$ (N_3O ligand) or two molar equivalents of Cu^{2+} to HL^{20} without base results in the formation of less than 8% of $[Cu(L^{20\cdot})(CH_3CN)]$. This low

yield for the Cu^{2+}-promoted oxidation reaction is consistent with an oxidation potential that is much higher for a phenol than for a phenolate group. Similar results were obtained when HL^{20} was replaced by HL^{30} (and also $[Cu(L^{20})(CH_3CN)]$ by $[Cu(L^{30})]_2$), thus showing that the nuclearity of the Cu^{II}-phenolate complex does not significantly influence the Cu^{2+}-promoted oxidation reaction.

A completely different behavior was observed upon treating HL^{37} and HL^{38} (ligand possessing a N_2O_2 donor set) with Cu^{2+}: as soon as copper is added a Cu^{II}-phenoxyl radical complex is formed in a disproportionation reaction.[63,66] The radical species $[Cu(L^{38\cdot})]_2$ is formed quantitatively in the presence of NEt_3 at two molar equivalent of added Cu^{2+}.[63] This species can also be formed in the absence of base, although it decomposes much faster. Addition of Cu^{2+} to $[Cu(L^{38\cdot})]_2$ results in the formation of a Cu^{II} bis(phenoxyl) species whose structure is proposed to be the monomeric complex $[Cu(L^{38\cdot\cdot})(CH_3CN)]$.

These results show that a change in the donor set of the ligand can direct the reaction from comproportionation towards disproportionation.

Ligands with N_2O_2 donor set:

$$2\ Cu^{II}\text{-}O \rightleftharpoons Cu^{II}\text{-}O^{\bullet} + \text{copper(I)}$$

Ligands with N_3O donor set:

$$2\ Cu^{II}\text{-}O \rightleftharpoons Cu^{II}\text{-}O^{\bullet} + \text{copper(I)}$$

A phenoxyl radical can thus be spontaneously formed by adding small amounts of Cu^{2+} to ligands possessing the same donor set as this enzyme.

Metamorphosing a GO's Reactivity by Using a Ligand Possessing a Five-Atom Donor Set

A ligand built on a triiminocyclohexane scaffold (H_2L^{54}; Figure 17) has been described by Walton et al.[99] The X-ray crystal structure of its copper(II) complex $[Cu(L^{54})]$ shows a pentacoordinate metal ion that resides in a square-pyramidal geometry as in GO. Unlike GO, however, which has a four-atom donor set with the fifth position vacant for substrate binding, no position seems to be available for substrate binding (and subsequent catalytic activity) in $[Cu(L^{54})]$ as the ligand already provides the five-atom donor set. Nevertheless, $[Cu(L^{54})]$ has been found to be active for the oxidation of benzyl alcohol (the substrate being added in its deprotonated alkoxide form) with molecular dioxygen as co-oxidant.[99] This result can be explained by considering the formation of an octahedral six-coordinate copper(II) complex in which the alcoholate is bound to the metal (see Figure 17).

Reactivity Studies

Several Cu^{II}-radical complexes have been found to be active towards oxidation of various substrates; we present here the reactivity of selected complexes belonging to each class. Theoretical approaches to catalytic mechanisms will be presented in the next chapter.

In 1996 Tolman et al. described $[Cu(L^{15})(CH_3CN)]$ as one of the first model complexes for the GO active site.[53] Bulk electrolysis of $[Cu(L^{15})(CH_3CN)]$ at a potential slightly higher than $E_{1/2}$ corresponding to the phenoxyl/phenolate redox couple affords a relatively stable Cu^{II}-phenoxyl radical complex. The electrochemical behavior of $[Cu(L^{15})$(benzyl alkoxide)] is characterized by a total loss of reversibility of the redox wave corresponding to the phenoxyl/phenolate couple (E_p^a = –0.01 V vs. Fc^+/Fc), as expected for an electrocatalytic process. In addition, bulk electrolysis of $[Cu(L^{15})$(benzyl alcoholate)] affords benzaldehyde in 46% yield, thus showing that the catalyst is only active as its Cu^{II}-phenoxyl radical form and that it exhibits a reactivity similar to that of GO towards the oxidation of alcohols.

The mononuclear Cu^{II}-diphenolate complex $[Cu(L^{11})]$ described by Wieghardt et al. catalyzes the aerobic oxidation of benzyl alcohol into benzaldehyde with a turnover number of 95 (24 h in the presence of catalytic amounts of base).[51] The proposed mechanism is similar to that reported for GO, in other words the active species is a Cu^{II}-phenoxyl radical species. In the presence of copper(I) and H_2L^{11}, primary amines with a least one α-H atom undergo an oxidative deamination reaction to yield Schiff base condensation products (17 turnovers in 24 h with benzylamine as substrate). The copper(II) complexes of H_2L^{11} are thus interesting examples of functional models for both GO and copper amine oxidase.

The copper(II) complex $[Cu(L^{12\cdot})]$ {and its zinc analog $[Zn(L^{12\cdot})]$} selectively oxidizes primary alcohols (methanol, ethanol, benzyl alcohol) stoichiometrically under anaerobic conditions in the presence of two equivalents of NEt_3 to yield the corresponding aldehyde, two equivalents of $HNEt_3^+$, and a protonated form of the two-electron-reduced catalyst (Figure 17, A).[46] No reaction was observed when using secondary alcohols such as 2-propanol or diphenylcarbinol, or when replacing $[Cu(L^{12\cdot})]$ with $[Cu(L^{12})]$. The mechanism involves reversible binding of an alkoxide ligand to $[Cu(L^{12\cdot})]$ to afford a five-coordinate, square-based-pyramidal complex where the axially bound phenolate is *cis* to the phenoxyl moiety (Figure 17, A). Irreversible oxidation of the substrate into a coordinated ketyl radical anion is the rate-determining step, with a remarkable KIE (k_H/k_D) of 54 for the reaction of methanol with $[Cu(L^{12\cdot})]$. The resulting intermediate is proposed to undergo a rapid intramolecular one-electron transfer, with the formation of aldehyde that dissociates. The ultimate electron acceptor is the *o*-diiminoquinone moiety of the doubly protonated ligand. The two-electron-reduced catalyst then reacts with molecular dioxygen to yield H_2O_2 in the presence of protons, thus regenerating $[Cu(L^{12\cdot})]$. A copper(II)-coordinated superoxide intermediate is proposed (Figure 17, A). Up to 5000 turnovers in 50 h are achieved for aerobic oxidation of methanol (turnover frequency of 0.03 s^{-1}). In contrast, the zinc analog is less efficient, with 170 turnovers achieved

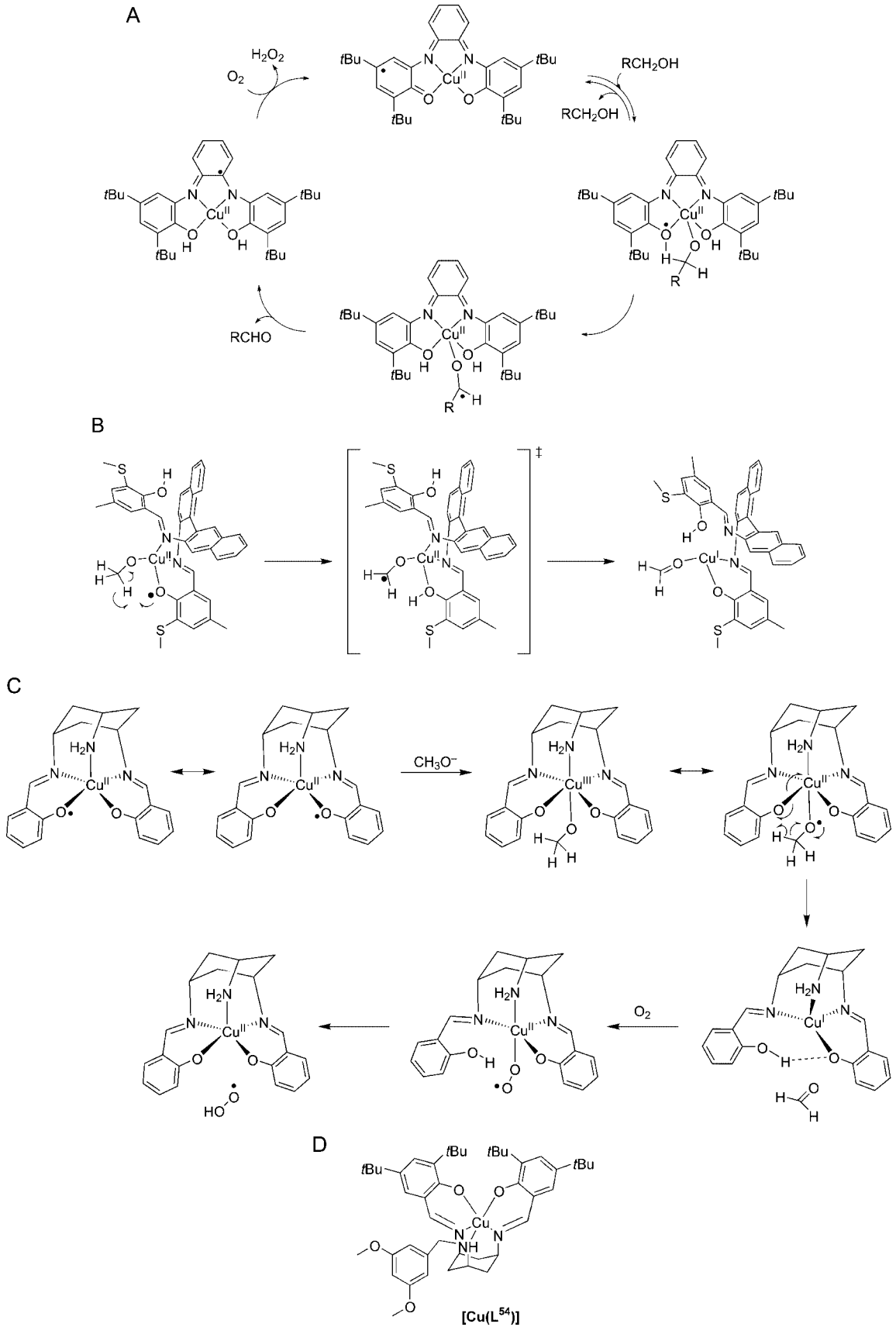

Figure 17. Proposed mechanisms for the catalytic oxidation of alcohols by [Cu($L^{12\cdot}$)] (A), and simplified models of [Cu(L^{2})] (B) and [Cu(L^{54})] (C) [adapted from ref.[46] (A), ref.[102,103] (B) and ref.[104] (C)]. The formula of [Cu(L^{54})] is also shown (D).

in 24 h (turnover frequency of 0.002 s^{-1}), which is attributed to a slower rate constant for hydrogen abstraction.

Itoh et al. have shown that [Cu($L^{27\cdot}$)(NO_3)] oxidizes benzyl alcohol stoichiometrically to benzaldehyde following pseudo-first-order kinetics.[100] The Cu^{I}-phenol complex of HL^{27} was recovered almost quantitatively at the end of reaction. In addition, a KIE of 8 was reported when α_D-benzyl alcohol was used, which shows that hydrogen abstraction is the rate-determining step in the reaction. [Cu($L^{27\cdot}$)(NO_3)] could thus be considered as a functional model of GO that stores two oxidative equivalents, one at the radical and the other at the copper(II) ion. It also stoichiometrically oxidizes phenols into phenoxyl radicals and 1,4-cyclohexadiene into benzene without a redox reaction at the metal center.[101] Phenol substrates are oxidized much faster than 1,4-cyclohexadiene in spite of the larger bond dissociation energy of the former. In addition, the steric effects of the phenol substituents are significant, with the reactivity order being 2,4,6-tri-*tert*-butylphenol < 2,6-di-*tert*-butylphenol < 2,4-di-*tert*-butylphenol. This strongly suggests that hydrogen atom abstraction from the phenol substrates is significantly enhanced by the coordinative interaction of the OH group to the metal ion center of the complex.

Yamauchi et al.[69] and ourselves[58,67] have reported that Cu^{II}-radical complexes of tripodal ligands possessing an N_2O_2 donor oxidize unactivated alcohols catalytically in the presence of small amounts of base. Using [Cu($HL^{39\cdot}$)(OAc)] as catalyst, 80 turnovers were achieved in one day for the oxidation of ethanol and 300 for the oxidation of benzyl alcohol, although the secondary alcohol cyclohexanol was not oxidized.[67] This catalyst thus reproduces the chemoselectivity of GO. A KIE was observed for the oxidation of benzyl alcohol, thereby suggesting that the rate-determining step is hydrogen abstraction. Hydrogen peroxide could not be detected, presumably due to its fast decomposition in the basic medium used, although its presence could be detected upon treating H_2L^{39} with CuCl.

Stack et al. have studied the reactivity of [Cu(L^6)] and [Cu(L^7)] with benzyl alcohol and 9,10-dihydroanthracene as substrates.[40] Regardless of the substrate or complex, the same overall stoichiometry of the reaction was observed: two equivalents of complex oxidize one equivalent of substrate, in other words the complex is effectively only a one-electron oxidant. More surprisingly, the reaction of benzyl alcohol with [Cu(L^6)] proceeds 10 times faster than with [Cu(L^7)] despite the fact that the former is a significantly weaker oxidant (ΔE = 0.37 V). These differences in rate constants have been interpreted as being due to mechanistic differences between the two reactions: The rate-determining step is a simple bimolecular reaction between [Cu(L^7)] and benzyl alcohol, while an associative mechanism involving a substrate-binding equilibrium prevails for the reaction of [Cu(L^6)] with $PhCH_2OH$. The opposite behavior was observed with 9,10-dihydroanthracene as substrate − the simple bimolecular reaction is observed between [Cu(L^6)] and 9,10-dihydroanthracene and the substrate-binding equilibrium preceding a unimolecular reaction in the reaction of [Cu(L^7)] with 9,10-dihydroanthracene. Reactions that include a substrate-binding equilibrium are faster than those occurring in simple bimolecular reactions due to the lowering of the entropic cost of the rate-determining steps induced by the substrate-binding equilibrium. The fact that saturation behavior could be observed for the reaction of [Cu(L^7)] with 9,10-dihydroanthracene indicates that the substrate-binding interaction is not associated with the presence of a polar hydroxyl group but may arise from either π–π stacking interactions or cation–π interactions (a high concentration of substrate may also change the solvent properties and thereby affect the reaction rates). 9,10-Dihydroanthracene reacts 25–300 times faster than benzyl alcohol, as expected for the lower bond dissociation energy of the former substrate. Large kinetic isotope effects were observed for all the substrates ($k_H/k_D > 5$) with a remarkable value of 19 for the reaction of [Cu(L^7)] with benzyl alcohol. These results show that the rate-determining step in the reaction is the homolytic cleavage of the C–H bond and that deprotonation of the alcoholic substrate probably does not occur prior to hydrogen atom abstraction. Results concerning the rate of reaction with 9,10-dihydroanthracene also indicate that the hydrogen atom abstraction abilities of the two Cu^{II}-phenoxyl species are comparable. The products of this hydrogen abstraction step are a highly reactive radical and the protonated form of the copper(II) complexes ([Cu(HL^6)] or [Cu(HL^7)]). The activation energies, and thus the rates for atom transfer reactions, were found to be correlated to the strength of the O(phenolate)–H bonds being formed in [Cu(HL^6)] and [Cu(HL^7)].

Complex [Cu($L^{6\cdot}$)] thus models the acceleration of the reaction rate upon substrate binding found in GO, although in the enzyme the acceleration is amplified by several orders of magnitude, presumably due to the formation of an extended hydrogen-bond network between the substrate and GO and deprotonation of the substrate by Tyr495 prior to hydrogen atom abstraction, which lowers the bond dissociation energy of its α-C–H bond.

Theoretical Approaches to Catalytic Mechanisms

Theoretical approaches to the oxidation of methoxide by [Cu($L^{2\cdot}$)][102,103] and [Cu($L^{54\cdot}$)][104] (in their Cu^{II}-phenoxyl radical form) have been undertaken. Ab initio molecular dynamics studies on [Cu($L^{2\cdot}$)] have shown that the methoxide adduct is a five-coordinate distorted pyramidal phenoxylcopper(II) complex.[102,103] The methoxide binds in the equatorial plane with a short Cu–O bond (1.93 Å), whereas the phenoxyl becomes an axial ligand with a much longer Cu–O bond (2.54 Å). This optimized structure is in good agreement with the EXAFS data. The unpaired electron switches from the axial to the equatorial position upon protonation of one phenolate (Figure 17, B). The p_z orbital hosting the unpaired electron in this structure is found to be orthogonal to the $d_{x^2-y^2}$ orbital of the copper.[103] In the transition state, the structural rearrangements are concentrated on the substrate, which moves towards the equatorial

oxygen. The unpaired electron that was previously located on the phenoxyl oxygen (and sulfur atom) mainly moves to the substrate, which may explain why this system only converts aromatic but not aliphatic alcohols. The electron transfer from the ketyl species to the copper ion then occurs spontaneously upon relaxation, thereby suggesting that hydrogen atom abstraction and electron transfer take place quasi-simultaneously, unlike in GO. A copper(I) compound is obtained as the product of the hydrogen atom abstraction step. Substantial geometric rearrangements are observed upon going from the transition state to this compound: one of the imine nitrogen moves away from the copper in such a way that the whole aromatic system (naphthyl and phenol) lies essentially in the same plane. The Cu^{I} ion in the resulting complex is tightly bound to one imine nitrogen and the aldehyde substrate, with one phenol oxygen being weakly bound as a third ligand. This suggests that release of the substrate is difficult and that molecular oxygen may bind when the aldehyde is still present.

DFT studies on [Cu($L^{54\cdot}$)] have revealed that substrate binding, as a sixth ligand, drives an intramolecular electron transfer that reduces the phenoxyl radical back to phenolate (Figure 17, C).[104] The substrate adduct is therefore formally an octahedral Cu^{III}-phenolate species, unlike in GO. This dramatic difference can be explained in terms of a proton transfer that occurs only in GO. Thus, after binding, the substrate transfers its alcohol proton to the axial tyrosinate Tyr495 residue that consequently coordinates only very weakly to afford an almost square-planar copper center (see part A of Figure 2, path 1). In [Cu($L^{54\cdot}$)], proton transfer leading to decoordination of a phenolate ring is prevented by the rigidity of the ligand framework and substrate binding generates an octahedral copper center instead. The substrate adduct of [Cu($L^{54\cdot}$)] also exhibits a large spin density on the methoxide oxygen, which indicates that it should be best formulated as lying between the Cu^{III}-OMe and Cu^{II}-$OMe^{\cdot}$ limits. In the hydrogen-transfer transition state, the SOMO is shifted to the carbon and rotated so that it points towards the phenolate oxygen. The barrier is 11.9 kcal mol^{-1} above that of GO (estimated with CH_3OH as substrate), which suggests a reduced activity of [Cu($L^{54\cdot}$)] relative to the enzyme and is consistent with a low turnover rate. A weakly bound Cu^{I}-aldehyde complex is obtained following the hydrogen atom and electron transfer, then the aldehyde is released and the metallic center is re-oxidized by molecular dioxygen into [Cu($L^{54\cdot}$)].

Bio-Inspired Systems

From Coordinated Mono- to Bis(phenoxyl) Radicals

Copper(II)-coordinated bis(phenoxyl) radicals have been described by Wieghardt et al. and ourselves with two types of ligands (TACN and salen).[37,56,57] This choice of ligand was dictated by the geometry of the copper(II) complexes: both phenolate moieties occupy the equatorial positions in the square-pyramidal copper(II)-TACN complex, while a square-planar (slightly distorted towards tetrahedral) environment is observed around the copper(II) ion in salen complexes [phenolate axial ligation consequently does not occur in any of these complexes, unlike copper(II) complexes of tripodal ligands].

The modular macrocycle TACN was used by Wieghardt et al.[56,57] The ligands $H_3L^{18,19}$ (Figure 5)[56] exhibit two one-electron transfer waves assigned to the successive oxidation of each phenolate moiety in their CV curve. The electrochemically generated Cu^{II}-phenoxyl complexes [Cu($HL^{18,19\cdot}$)] and [Cu($HL^{18,19\cdot}$)] could be obtained, but it was not possible to obtain the diradical form of [Cu($HL^{18,19\cdot}$)] even by performing controlled potential electrolysis at 243 K. The diradical complex [Cu($L^{17\cdot\cdot}$)] (Figure 18) could be obtained from the ligand H_2L^{17}.[57] It exhibits signals in the broad field range at effective g factors close to 5 and 3 in its EPR spectrum. This spectrum has been interpreted by considering a ferromagnetic coupling of Cu^{II} and each of the radicals that dominates the weaker antiferromagnetic radical–radical interaction. Simulation yielded a large D value of 0.4 cm^{-1}, in agreement with a strong dipolar interaction between the Cu^{II} and coordinated phenoxyl radicals. This situation thus contrasts sharply with that of the Cu^{II}-bis(iminosemiquinonate) diradical complex [Cu($L^{12\cdot\cdot}$)], which exhibits an S = 1/2 ground state.[46]

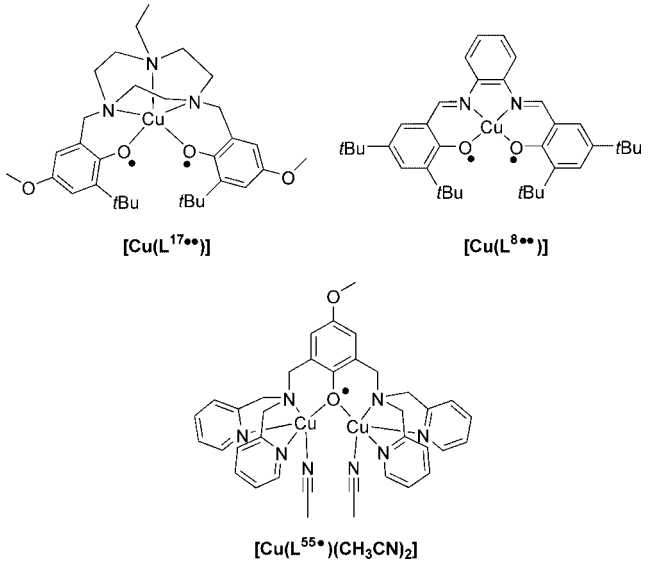

Figure 18. Bio-inspired system formally storing three oxidizing equivalents: [Cu($L^{17\cdot\cdot}$)] (ref.[57]), [Cu($L^{8\cdot\cdot}$)] (ref.[37]), [Cu($L^{55\cdot}$)-$(CH_3CN)_2$] (ref.[73]).

In another approach we have used salen-type ligands to study the respective influence of the hybridization of the nitrogens and flexibility of the linker between these two atoms on the properties of the electrogenerated Cu^{II}-phenoxyl and Cu^{II}-bis(phenoxyl) radical complexes (Figure 18).[37] The copper(II) complexes used are those of H_2L^3, H_2L^5, and $H_2L^{7,8}$ (Figure 3). While [Cu(L^7)] and [Cu(L^8)] incorporate a rigid linker, [Cu(L^3)] and [Cu(L^5)] contain a flexible one. The geometry around the metal ion is planar for [Cu(L^5)] and [Cu(L^8)] while it is slightly distorted towards tetrahedral for [Cu(L^3)] and [Cu(L^7)].

The electrochemically generated monoradical species [Cu(L$^{3\cdot}$)], [Cu(L$^{5\cdot}$)], and [Cu(L$^{7,8\cdot}$)] are relatively stable and X-band EPR-silent at 4–100 K, similar to other Cu^{II}-phenoxyl salen complexes,[34,35,39,43] thereby indicating that the phenoxyl moiety remains coordinated to the copper atom. The two-electron-oxidized species exhibit X-band EPR spectra that depend strongly on the ligand structure. The EPR spectra of [Cu(L$^{7\cdot\cdot}$)] and [Cu(L$^{8\cdot\cdot}$)] at 4 K exhibit signals that are distributed over the entire spectral width, similar to the Cu^{II}-bis(phenoxyl) radical complex [Cu(L$^{17\cdot\cdot}$)] described by Wieghardt et al.[57] A similar electronic structure is thus proposed, in other words a dominant ferromagnetic coupling between the Cu^{II} and each of the radicals that yields large D values. The EPR spectra of [Cu(L$^{3\cdot\cdot}$)] and [Cu(L$^{5\cdot\cdot}$)] are completely different as they are the superposition of two spectra, one typical of an organic radical (narrow signal at g = 2.005) and the other corresponding to a mononuclear copper(II) complex. The ethyl linker is thus too flexible to maintain both phenoxyl moieties coordinated to the metal ion. The rigid linkers prevent decomplexation, regardless of whether the geometry around the metal center is planar {[Cu(L$^{8\cdot\cdot}$)]} or distorted towards tetrahedral {[Cu(L$^{7\cdot\cdot}$)]}.

A Bridging Phenoxyl Radical in Dicopper(II) Complexes

In order to get a μ-phenoxyldicopper(II) system, a building block comprising at least one μ-phenolatedicopper(II) entity has to be oxidized. As discussed above, tripodal ligands show a marked tendency to assemble as dimers (of formula [Cu(L^{N_3O})]$_2$ and [Cu(L^{N_2O_2})]$_2$) that possess such a core when the steric bulk at the *o*-position of the phenolate is small to moderate (Figure 7). Unfortunately, we have shown that oxidation of [Cu(L^{30,31})]$_2$ affords the corresponding mononuclear [Cu(L$^{30,31\cdot}$)(CH$_3$CN)] species,[63] while oxidation of [Cu(L^{38,41})]$_2$ takes place at the nonbridging phenolate group to afford dimeric structures [Cu(L$^{38,41\cdot}$)]$_2$ with two Cu^{II}-phenoxyl radical molecules bridged by phenolato groups.[58,69] We have therefore synthesized the dicopper(II) complexes of the dinucleating ligand HL^{55}.[73] Two complexes were isolated, whose structures depend on the amount of NEt$_3$ added during the synthesis. [Cu(L^{55})(CH$_3$CN)$_2$] was obtained in the presence of a single equivalent. This complex contains two copper(II) atoms with square-pyramidal geometries that are coordinated to one μ-phenolate oxygen and three nitrogens from the ligand, and one nitrogen from an exogenous acetonitrile molecule. The metal centers are separated by 4.059(5) Å and interact magnetically, as shown by the spin triplet resonance in the EPR spectrum of this complex. [Cu(L^{55})(μ-OH)] was isolated when two molar equivalents of NEt$_3$ were used. Its structure differs from that of [Cu(L^{55})(CH$_3$CN)$_2$] in several points: the geometry around the copper atom is trigonal bipyramidal, the exogenous acetonitrile ligands are replaced by a single μ-OH molecule, and the intermetallic distance is much shorter [2.980(9) Å]. Consequently, the interaction between the copper(II) atoms in [Cu(L^{55})(μ-OH)] is strongly antiferromagnetic, as opposed to the ferromagnetic interaction observed in [Cu(L^{55})(CH$_3$CN)$_2$]. These two complexes are oxidized to the μ-phenoxyl radical species [Cu(L$^{55\cdot}$)(μ-OH)] and [Cu(L$^{55\cdot}$)(CH$_3$CN)$_2$] over the same potential range (0.36–0.45 V). The former was found to be much less stable than the latter (the half-lives are <20 s and 22.3 min, respectively, at 298 K), thus showing that the reactivity is finely tuned by the nature of the coordinating ligand. The EPR spectrum of the most stable complex [Cu(L$^{55\cdot}$)(CH$_3$CN)$_2$] at 4 K exhibits a $\Delta M_S = \pm 3$ transition at g = 8 that is the signature of an S = 3/2 system. Its temperature dependence shows that it corresponds to the ground state. The D value (–0.056 cm^{-1}) is close to that reported for an excited S = 3/2 spin state in a triangular tricopper(II) system, but much higher than those reported for triradicals and lower than those reported for copper(II)-coordinated bis(phenoxyl) radicals. Since tyrosyl radicals are ubiquitous in metalloenzymes, such species could be biologically relevant. In addition, Karlin et al. have recently proposed the involvement of such species in a ligand cross-linking reaction promoted by a hydroperoxidodicopper(II) complex.[105]

Conclusions

The biomimetic approach to the GO active site developed concomitantly by a number of research groups has led to the synthesis and characterization of a wide range of Cu^{II}-phenoxyl complexes. Enormous progress has thus been made from an entity that was unknown in coordination chemistry ten years ago. Many features of the GO active site have been reproduced successfully, providing valuable information on its spectroscopic signature, structure, and even reactivity. Replication of its oxidative chemistry has been achieved, although this reactivity is limited compared to that of the enzyme. Recent results in this field concerning bio-inspired complexes of aminyl radical ligands[106,107] or theoretical calculations[108] suggest that a catalytic efficiency approaching that of the enzyme is conceivable. This bio-inorganic story concerning coordinated radicals is thus far from finished, and the number of articles concerning radical metalloenzymes, specifically new copper(II)-radical metalloenzymes,[109–111] and metal-radical complexes will increase further in the near future.

Acknowledgments

I am grateful to Prof. J.-L. Pierre for his interest in this work and fruitful discussions.

[1] J. L. Pierre, *Chem. Soc. Rev.* **2000**, *29*, 251–257.
[2] J. A. Stubbe, W. Van Der Donk, *Chem. Rev.* **1998**, *98*, 705–762.
[3] M. S. Rodgers, D. M. Dooley, *Curr. Opin. Chem. Biol.* **2003**, *7*, 189–196.
[4] M. Fontecave, J. L. Pierre, *Bull. Soc. Chim. Fr.* **1996**, *133*, 653–660.
[5] B. A. Jazdzewski, W. B. Tolman, *Coord. Chem. Rev.* **2000**, *200–202*, 633–685.

[6] S. Itoh, M. Taki, S. Fukuzumi, *Coord. Chem. Rev.* **2000**, *198*, 3–20.
[7] P. Chaudhuri, K. Wieghardt, *Prog. Inorg. Chem.* **2001**, *50*, 151–216.
[8] P. Chaudhuri, K. Wieghardt, T. Weyhermüller, T. K. Paine, S. Mukherjee, C. Mukherjee, *Biol. Chem.* **2005**, *386*, 1023–1033.
[9] C. D. Borman, C. G. Saysell, A. Sokolowski, M. B. Twitchett, C. Wright, A. G. Sykes, *Coord. Chem. Rev.* **1999**, *190–192*, 771–779.
[10] M. J. McPherson, M. R. Parsons, R. K. Spooner, C. M. Wilmot, *Handbook of Metalloproteins*, John Wiley and Sons, Chichester, **2001**, 1272–1283.
[11] J. W. Whittaker, *Chem. Rev.* **2003**, *103*, 2347–2363.
[12] N. Ito, S. E. V. Philips, C. Stevens, Z. B. Ogel, M. J. McPherson, J. N. Keen, K. D. S. Yadav, P. F. Knowles, *Nature* **1991**, *350*, 87–90.
[13] N. Ito, S. E. V. Philips, K. D. S. Yadav, P. F. Knowles, *J. Mol. Biol.* **1994**, *238*, 794–814.
[14] In order to facilitate comparison between the systems, all electrochemical potentials are given relative to the Fc^+/Fc reference. When potentials have been reported relative to other standards, corrections are applied according to the following references: N. G. Connelly, W. E. Geiger, *Chem. Rev.* **1996**, *96*, 877–910; V. V. Pavlishchuk, A. W. Addison, *Inorg. Chim. Acta* **2000**, *298*, 97–102. Differences in solvent, electrolyte, and ionic strength may, however, complicate the comparison.
[15] C. Wright, A. G. Sykes, *J. Inorg. Biochem.* **2001**, *85*, 237–243.
[16] M. M. Whittaker, C. A. Ekberg, J. Peterson, M. S. Sendova, E. P. Day, J. W. Whittaker, *J. Mol. Catal. B* **2000**, *8*, 3–15.
[17] D. Rokhsana, D. M. Dooley, R. K. Szilagyi, *J. Am. Chem. Soc.* **2006**, ASAP.
[18] M. M. Whittaker, J. W. Whittaker, *J. Biol. Chem.* **1988**, *263*, 6074–6080.
[19] M. M. Whittaker, D. P. Ballou, J. W. Whittaker, *Biochemistry* **1998**, *37*, 8426–8436.
[20] B. P. Branchaud, M. P. Montague-Smith, D. J. Kosman, F. R. McLaren, *J. Am. Chem. Soc.* **1993**, *115*, 798–800.
[21] R. M. Wachter, B. P. Branchaud, *Biochim. Biophys. Acta* **1998**, *1384*, 43–54.
[22] M. M. Whittaker, J. W. Whittaker, *Biophys. J.* **1993**, *64*, 762–772.
[23] F. Himo, L. A. Eriksson, F. Maseras, P. E. M. Siegbahn, *J. Am. Chem. Soc.* **2000**, *122*, 8031–8036.
[24] B. E. Turner, B. P. Branchaud, *Bioorg. Med. Chem. Lett.* **1999**, *9*, 3341–3346.
[25] R. M. Wachter, B. P. Branchaud, *Biochim. Biophys. Acta* **1998**, *1384*, 43–54.
[26] M. M. Whittaker, J. W. Whittaker, *Biochemistry* **2001**, *40*, 7140–7148.
[27] S. G. Minasian, M. M. Whittaker, J. W. Whittaker, *Biochemistry* **2004**, *43*, 13683–13693.
[28] S. J. Firbank, M. S. Rogers, C. M. Wilmot, D. M. Dooley, M. A. Halcrow, P. F. Knowles, M. J. McPherson, S. E. V. Phillips, *Proc. Natl. Acad. Sci. USA* **2001**, *98*, 12932–12937.
[29] M. S. Rogers, A. J. Baron, M. J. McPherson, P. F. Knowles, D. M. Dooley, *J. Am. Chem. Soc.* **2000**, *122*, 990–991.
[30] M. M. Whittaker, J. W. Whittaker, *J. Biol. Chem.* **2003**, *278*, 22090–22101.
[31] E. R. Altwicker, *Chem. Rev.* **1967**, *67*, 475–531.
[32] J. G. Radziszewski, M. Gil, A. Gorski, J. Spanget-Larsen, J. Waluk, B. J. Mroz, *J. Chem. Phys.* **2001**, *115*, 9733–9738.
[33] N. Katajima, K. Whang, Y. Moro-Oka, A. Uchida, Y. Sasada, *J. Chem. Soc., Chem. Commun.* **1986**, 1504–1505.
[34] Y. Wang, T. D. P. Stack, *J. Am. Chem. Soc.* **1996**, *118*, 13097–13098.
[35] Y. Wang, J. L. Dubois, B. Hedman, K. O. Hodgson, T. D. P. Stack, *Science* **1998**, *279*, 537–540.
[36] E. Saint-Aman, S. Ménage, J.-L. Pierre, E. Defrancq, G. Gellon, *New J. Chem.* **1998**, *22*, 393–394.
[37] F. Thomas, O. Jarjayes, C. Duboc, C. Philouze, E. Saint-Aman, J.-L. Pierre, *Dalton Trans.* **2004**, 2662–2669.
[38] M. Vaidyanathan, M. Palaniandavar, R. S. Gopalan, *Ind. J. Chem.* **2003**, *42A*, 2210–2222.
[39] R. C. Pratt, T. D. P. Stack, *J. Am. Chem. Soc.* **2003**, *125*, 8716–8717.
[40] R. C. Pratt, T. D. P. Stack, *Inorg. Chem.* **2005**, *44*, 2367–2375.
[41] I. Sylvestre, J. Wolowska, C. A. Kilner, E. J. L. McInnes, M. A. Halcrow, *Dalton Trans.* **2005**, 3241–3249.
[42] Y. Pellegrin, A. Quaranta, P. Dorlet, M.-F. Charlot, W. Leibl, A. Aukauloo, *Chem. Eur. J.* **2005**, *11*, 3698–3710.
[43] A. dos Anjos, A. J. Bortoluzzi, R. E. H. M. B. Osorio, R. A. Peralta, G. R. Friedermann, A. S. Mangrich, A. Neves, *Inorg. Chem. Commun.* **2005**, *8*, 249–253.
[44] P. Chaudhuri, M. Hess, U. Flörke, K. Wieghardt, *Angew. Chem.* **1998**, *110*, 2340–2343; *Angew. Chem. Int. Ed.* **1998**, *37*, 2217–2220.
[45] P. Chaudhuri, M. Hess, T. Weyhermüller, K. Wieghardt, *Angew. Chem.* **1999**, *111*, 1165–1168; *Angew. Chem. Int. Ed.* **1999**, *38*, 1095–1098.
[46] P. Chaudhuri, M. Hess, J. Müller, K. Hildenbrandt, E. Bill, T. Weyhermüller, K. Wieghardt, *J. Am. Chem. Soc.* **1999**, *121*, 9599–9610.
[47] P. Chaudhuri, C. N. Nazari, E. Bill, E. Bothe, T. Weyhermüller, K. Wieghardt, *J. Am. Chem. Soc.* **2001**, *123*, 2213–2223.
[48] T. Kruse, T. Weyhermüller, K. Wieghardt, *Inorg. Chim. Acta* **2002**, *331*, 81–89.
[49] S. Mukherjee, E. Rentschler, T. Weyhermüller, K. Wieghardt, P. Chaudhuri, *Chem. Commun.* **2003**, 1828–1829.
[50] K. S. Min, T. Weyhermüller, E. Bothe, K. Wieghardt, *Inorg. Chem.* **2004**, *43*, 2922–2931.
[51] T. K. Paine, T. Weyhermüller, K. Wieghardt, P. Chaudhuri, *Dalton Trans.* **2004**, 2092–2101.
[52] J. Müller, T. Weyhermüller, E. Bill, P. Hildebrandt, L. Ould-Moussa, T. Glaser, K. Wieghardt, *Angew. Chem.* **1998**, *110*, 637–640; *Angew. Chem. Int. Ed.* **1998**, *37*, 616–619.
[53] J. A. Halfen, V. G. Young Jr, W. B. Tolman, *Angew. Chem.* **1998**, *108*, 1832–1835; *Angew. Chem. Int. Ed. Engl.* **1996**, *35*, 1687–1690.
[54] J. A. Halfen, B. A. Jazdzewski, S. Mahapatra, L. M. Berreau, E. C. Wilkinson, L. Que Jr, W. B. Tolman, *J. Am. Chem. Soc.* **1997**, *119*, 8217–8227.
[55] B. A. Jazdzewski, A. M. Reynolds, P. L. Holland, V. G. Young Jr, S. Kaderli, A. D. Zuberbühler, W. B. Tolman, *J. Biol. Inorg. Chem.* **2003**, *8*, 381–393.
[56] A. Sokolowski, H. Leutbecher, T. Weyhermüller, R. Schnepf, E. Bothe, E. Bill, P. Hildebrandt, K. Wieghardt, *J. Biol. Inorg. Chem.* **1997**, *2*, 444–453.
[57] E. Bill, J. Müller, T. Weyhermüller, K. Wieghardt, *Inorg. Chem.* **1999**, *38*, 5795–5802.
[58] A. Philibert, F. Thomas, C. Philouze, S. Hamman, E. Saint-Aman, J. L. Pierre, *Chem. Eur. J.* **2003**, *9*, 3803–3812.
[59] Y. Shimazaki, S. Huth, S. Hirota, O. Yamauchi, *Bull. Chem. Soc. Jpn.* **2000**, *73*, 1187–1195.
[60] F. Michel, F. Thomas, C. Philouze, S. Hamman, E. Saint-Aman, J. L. Pierre, unpublished results.
[61] S. Itoh, M. Taki, H. Kumei, S. Takayama, S. Nagatomo, T. Kitagawa, N. Sakurada, R. Arakawa, S. Fukuzumi, *Inorg. Chem.* **2000**, *39*, 3708–3711.
[62] M. Taki, H. Hattori, T. Osako, S. Nagatomo, M. Shiro, T. Kitagawa, S. Itoh, *Inorg. Chim. Acta* **2004**, *357*, 3369–3381.
[63] F. Michel, F. Thomas, S. Hamman, E. Saint-Aman, C. Bucher, J. L. Pierre, *Chem. Eur. J.* **2004**, *10*, 4115–4125.
[64] F. Michel, S. Hamman, F. Thomas, C. Philouze, I. Gautier-Luneau, J. L. Pierre, *Chem. Commun.* **2006**, 4122–4124.
[65] D. Zurita, I. Gautier-Luneau, S. Ménage, J. L. Pierre, E. Saint-Aman, *J. Biol. Inorg. Chem.* **1997**, *2*, 46–55.
[66] Y. Shimazaki, S. Huth, A. Odani, O. Yamauchi, *Angew. Chem.* **2000**, *112*, 1732–1735; *Angew. Chem. Int. Ed.* **2000**, *39*, 1666–1669.

[67] F. Thomas, G. Gellon, I. Gautier-Luneau, E. Saint-Aman, J. L. Pierre, *Angew. Chem.* **2002**, *114*, 3173–3176; *Angew. Chem. Int. Ed.* **2002**, *41*, 3047–3050.
[68] M. Taki, H. Kumei, S. Nagatomo, T. Kitagawa, S. Itoh, S. Fukuzumi, *Inorg. Chim. Acta* **2000**, *300–302*, 622–632.
[69] Y. Shimazaki, S. Huth, S. Hirota, O. Yamauchi, *Inorg. Chim. Acta* **2002**, *331*, 168–177.
[70] The value of τ is zero for a perfect square pyramid and unity for a trigonal bipyramid. See: A. W. Addison, T. N. Rao, J. Reedijk, J. van Rijn, G. C. Verschoor, *J. Chem. Soc., Dalton Trans.* **1984**, 1349–1356.
[71] H. Adams, N. A. Bailey, I. K. Campbell, D. E. Fenton, Q.-Y. He, *J. Chem. Soc., Dalton Trans.* **1996**, 2233–2237.
[72] M. Vaidyanathan, R. Viswanathan, M. Palaniandavar, T. Balasubramanian, P. Prabhaharan, T. P. Muthiah, *Inorg. Chem.* **1998**, *37*, 6418–6427.
[73] F. Michel, S. Torelli, F. Thomas, C. Duboc, C. Philouze, C. Belle, S. Hamman, E. Saint-Aman, J. L. Pierre, *Angew. Chem.* **2005**, *117*, 442–445; *Angew. Chem. Int. Ed.* **2005**, *44*, 438–441.
[74] S. Itoh, S. Takayama, R. Arakawa, A. Furuta, M. Komatsu, A. Ishida, S. Takamuku, S. Fukuzumi, *Inorg. Chem.* **1997**, *36*, 1407–1416.
[75] D. Zurita, C. Scheer, J. L. Pierre, E. Saint-Aman, *J. Chem. Soc., Dalton Trans.* **1996**, 4331–4336.
[76] C. Ochs, F. E. Hahn, R. Fröhlich, *Eur. J. Inorg. Chem.* **2001**, 2427–2436.
[77] A. J. Bard, L. R. Faulkner, *Electrochemical Methods, Fundamentals and Applications*, Wiley, New York, **1980**.
[78] K. Yamato, T. Inada, M. Doe, A. Ichimura, T. Takui, Y. Kojima, T. Kikunaga, N. Yanagihara, T. Onaka, S. Yano, *Bull. Chem. Soc. Jpn.* **2000**, *73*, 903–912.
[79] A. Berkessel, M. Doucet, S. Bulat, K. Glaubitz, *Biol. Chem.* **2005**, *386*, 1035–1041.
[80] M. A. Hossain, F. Thomas, S. Hamman, E. Saint-Aman, D. Boturyn, P. Dumy, J.-L. Pierre, *J. Pept. Sci.* **2006**, *12*, 612–619.
[81] O. Sénèque, M. Campion, B. Douziech, M. Giorgi, Y. Le Mest, O. Reinaud, *Dalton Trans.* **2003**, 4216–4218.
[82] M. L. McGlashen, D. D. Eads, T. Spiro, J. W. Whittaker, *J. Phys. Chem.* **1995**, *99*, 4918–4922.
[83] M. A. Halcrow, L. M. L. Chia, X. Liu, E. J. L. McInnes, L. J. Yellowlees, F. E. Mabbs, J. E. Davies, *Chem. Commun.* **1998**, 2465–2466.
[84] M. A. Halcrow, L. M. L. Chia, X. Liu, E. J. L. McInnes, L. J. Yellowlees, F. E. Mabbs, I. J. Scowen, M. McPartlin, J. E. Davies, *J. Chem. Soc., Dalton Trans.* **1999**, 1753–1762.
[85] R. C. Pratt, L. M. Mirica, T. D. P. Stack, *Inorg. Chem.* **2004**, *43*, 8030–8039.
[86] X. Liu, E. J. L. McInnes, C. A. Kilner, M. Thornton-Pett, M. A. Halcrow, *Polyhedron* **2001**, *20*, 2889–2900.
[87] X. Liu, S. A. Barrett, C. A. Kilner, M. Thornton-Pett, M. A. Halcrow, *Tetrahedron* **2002**, *58*, 603–611.
[88] M. A. Halcrow, E. J. L. McInnes, F. E. Mabbs, I. J. Scowen, M. McPartlin, H. R. Powell, J. E. Davies, *J. Chem. Soc., Dalton Trans.* **1997**, 4025–4035.
[89] M. A. Halcrow, N. L. Cromhout, P. R. Raithby, *Polyhedron* **1997**, *16*, 4257–4264.
[90] X. Liu, L. M. L. Chia, C. A. Kilner, L. J. Yellowlees, M. Thornton-Pett, S. Trofimenko, M. A. Halcrow, *Chem. Commun.* **2000**, 1947–1948.
[91] R. Uma, R. Viswanathan, M. Palaniandavar, M. Lakshminarayanan, *J. Chem. Soc., Dalton Trans.* **1994**, 1219–1226.
[92] H. Adams, N. A. Bailey, C. O. Rodriguez de Barbarin, D. E. Fenton, Q.-Y. He, *J. Chem. Soc., Dalton Trans.* **1995**, 2323–2331.
[93] F. Michel, F. Thomas, S. Hamman, C. Philouze, E. Saint-Aman, J.-L. Pierre, *Eur. J. Inorg. Chem.* **2006**, 3684–3696.
[94] K. D. Karlin, B. I. Cohen, J. C. Hayes, A. Farooq, J. Zubieta, *Inorg. Chem.* **1987**, *26*, 147–153.
[95] For recent articles see: S. Mukherjee, E. Rentschler, T. Weyhermüller, K. Wieghardt, P. Chaudhuri, *Chem. Commun.* **2003**, 1828–1829; K. Sik Min, T. Weyhermüller, K. Wieghardt, *Dalton Trans.* **2003**, 1126–1132; S. Mukherjee, T. Weyhermüller, K. Wieghardt, P. Chaudhuri, *Dalton Trans.* **2003**, 3483–3485; P. Ghosh, E. Bill, T. Weyhermüller, K. Wieghardt, *J. Am. Chem. Soc.* **2003**, *125*, 3967–3979; K. Sik Min, T. Weyhermüller, K. Wieghardt, *Dalton Trans.* **2004**, 178–186; S. Mukherjee, T. Weyhermüller, E. Bothe, K. Wieghardt, P. Chaudhuri, *Dalton Trans.* **2004**, 3842–3853; K. S. Min, T. Weyhermüller, E. Bothe, K. Wieghardt, *Inorg. Chem.* **2004**, *43*, 2922–2931; K. Chlopek, E. Bill, T. Weyhermüller, F. Neese, K. Wieghardt, *Inorg. Chem.* **2005**, *44*, 3636–3656; C. Mukherjee, T. Weyhermüller, K. Wieghardt, P. Chaudhuri, *Dalton Trans.* **2006**, 2169–2171; K. Chlopek, E. Bothe, F. Neese, T. Weyhermüller, K. Wieghardt, *Inorg. Chem.* **2006**, *45*, 6298–6307.
[96] A. Sokolowski, E. Bothe, E. Bill, T. Weyhermüller, K. Wieghardt, *Chem. Commun.* **1996**, 1671–1672.
[97] L. Benisvy, A. J. Blake, D. Collison, E. S. Davies, C. D. Garner, E. J. L. McInnes, J. McMaster, G. Whittaker, C. Wilson, *Chem. Commun.* **2001**, 1824–1825.
[98] L. Benisvy, A. J. Blake, D. Collison, E. S. Davies, C. D. Garner, E. J. L. McInnes, J. McMaster, G. Whittaker, C. Wilson, *Dalton Trans.* **2003**, 1975–1985.
[99] A. K. Nairn, S. J. Archibald, R. Bhalla, B. C. Gilbert, E. J. MacLean, S. J. Teat, P. H. Walton, *Dalton Trans.* **2006**, *1*, 172–176.
[100] S. Itoh, M. Taki, S. Takayama, S. Nagatomo, T. Kitagawa, N. Sakurada, R. Arakawa, S. Fukuzumi, *Angew. Chem.* **1999**, *111*, 2944–2946; *Angew. Chem. Int. Ed.* **1999**, *38*, 2774–2776.
[101] M. Taki, H. Kumei, S. Itoh, S. Fukuzumi, *J. Inorg. Biochem.* **2000**, *78*, 1–5.
[102] U. Rothlisberger, P. Carloni, *Int. J. Quant. Chem.* **1999**, *73*, 209–218.
[103] U. Rothlisberger, P. Carloni, K. Doclo, M. Parrinello, *J. Biol. Inorg. Chem.* **2000**, *5*, 236–250.
[104] E. Zueva, P. H. Walton, J. E. McGrady, *Dalton Trans.* **2006**, *1*, 159–167.
[105] L. Li, N. Sarjeant, K. D. Karlin, *Inorg. Chem.* **2006**, *45*, 7160–7172.
[106] T. Büttner, J. Geier, G. Frison, J. Harmer, C. Calle, A. Schweiger, H. Schönberg, H. Grützmacher, *Science* **2005**, *307*, 235–238.
[107] H. Grützmacher, personal communication.
[108] L. Guidoni, K. Spiegel, M. Zumstein, U. Röthlisberger, *Angew. Chem.* **2004**, *116*, 3348–3351; *Angew. Chem. Int. Ed.* **2004**, *43*, 3286–3289.
[109] M. M. Whittaker, P. J. Kersten, N. Nakamura, J. Sandres-Loehr, E. S. Schweizer, J. W. Whittaker, *J. Biol. Chem.* **1996**, *271*, 681–687.
[110] M. M. Whittaker, P. J. Kersten, D. Cullen, J. W. Whittaker, *J. Biol. Chem.* **1999**, *274*, 36226–36232.
[111] M. M. Whittaker, J. W. Whittaker, *Arch. Biochem. Biophys.* **2006**, *452*, 108–118.

Received: November 21, 2006
Published Online: April 13, 2007

